A Unified Mathematical Theory of Energy-Efficient AI: Thermodynamic, Information-Theoretic, and Spectral Foundations for Sustainable Large-Scale Machine Learning

Da Xu
China Mobile Research Institute
xuda@chinamobile.com

December 3, 2025

Abstract

The exponential growth in computational requirements for large AI models—from GPT-4's estimated $\sim$1.8×10^{25} FLOPs training cost (based on public reports and scaling law extrapolations; actual values undisclosed) to the projected zettaFLOP-scale models of 2030—demands a rigorous theoretical foundation for energy-efficient machine learning. We develop a unified mathematical framework connecting five fundamental perspectives: **(i)** thermodynamic bounds rooted in Landauer's principle; **(ii)** information-theoretic limits from rate-distortion and channel capacity; **(iii)** spectral graph theory governing attention mechanisms; **(iv)** Riemannian geometry of optimization landscapes; and **(v)** non-equilibrium statistical mechanics of training dynamics.

Our core theoretical contributions establish:

- **Fundamental Energy-Accuracy Trade-off** (Theorem 3.3): For any learning algorithm achieving error ϵ, the minimum energy scales as $\mathrm{E}^*(\epsilon) = \Omega\big(k_B T \cdot p \cdot \log(1/\epsilon)\big)$, where p is the effective parameter count.
- **Scaling Laws from First Principles** (Theorem 4.3): We derive $\mathrm{E}(n, p, s) = \Theta(p \cdot s^\beta \cdot n^{-\alpha})$ from thermodynamic and information-theoretic axioms, explaining empirical Chinchilla-style scaling.
- **Latency-Energy-Throughput Trilemma** (Theorem 4.2): Any inference system satisfies Latency × Energy × $\text{Throughput}^{-1} \geq \Omega(p \cdot d \cdot k_B T)$.
- **Attention Energy Lower Bound** (Theorem 3.10): Computing attention over N tokens requires $\mathrm{E} \geq \Omega(N \cdot d \cdot k_B T \ln 2)$ bits of irreversible information processing.

As a constructive application, we develop **Spectral Sparse Attention (SSA)**, achieving $O(N^{1.5})$ complexity with provable spectral preservation guarantees (Theorem 9.4). Our theory predicts substantial energy reductions for long-context scenarios; preliminary experiments on synthetic clustered data demonstrate 2× speedup at $N = 4096$ with gradient direction preservation (cosine similarity > 0.76). While full validation on production language modeling benchmarks remains future work, the theoretical framework provides principled guidance for the next generation of sustainable AI systems.

1 Introduction

1.1 The Energy Crisis in Modern AI

The computational cost of training and deploying large language models has grown exponentially, with energy consumption emerging as a critical constraint for sustainable AI development. Training GPT-4 class models is estimated to consume megawatt-hours of electricity, and inference at scale presents equally daunting energy challenges. Consider the scale of modern AI systems:

This motivates a fundamental question: *What are the theoretical limits of energy-efficient AI, and how can we design algorithms that approach these limits?*

Model	Parameters	Training FLOPs	Est. Energy (MWh)
GPT-3	175B	3.1×10^{23}	1,300
GPT-4 (est.)[†]	1.8T MoE	1.8×10^{25}	51,000
LLaMA-2 70B	70B	1.7×10^{24}	7,200
Gemini Ultra (est.)	>1T	$> 10^{25}$	>50,000

Table 1: Energy footprint of frontier AI models. Energy estimates assume H100 GPUs at 700W with 50% utilization and 10^{15} FLOPs/s throughput. [†]GPT-4 estimates based on public reports and scaling law extrapolations [11]; actual values are not officially disclosed.

1.2 The Core Challenge: Attention Complexity

The self-attention mechanism, defined as $A(Q, K, V) = \text{softmax}(\frac{QK^T}{\sqrt{d}})V$, exemplifies this challenge. Mathematically, it represents a fully connected graph $\mathcal{G}$ where every token attends to every other token, incurring $O(N^2)$ computational cost that is physically unsustainable for long-context reasoning.

Example 1.1 (Energy Cost of Long-Context Attention). For a 175B parameter model processing 32K tokens:

- Dense attention FLOPs: $2 \cdot N^2 \cdot d \cdot L = 2 \cdot 32768^2 \cdot 12288 \cdot 96 \approx 2.5 \times 10^{15}$ per forward pass
- At 700W and 3×10^{14} FLOPs/s: $\approx$19.4 Joules per inference
- At 1M queries/day: $19.4 \times 10^6 \times 365 \approx 7.1$ GJ/year ≈ 2.0 MWh/year just for attention computation

Reducing attention complexity by 50% saves $\approx$1.0 MWh/year—equivalent to powering 90 US homes for a day.

1.3 A Systematic Theory: Five Pillars

We argue that addressing energy efficiency requires a *principled theoretical framework* that unifies five fundamental perspectives:

1. **Thermodynamics (Section 3.1):** Landauer's principle establishes $k_B T \ln 2$ as the minimum energy per bit erasure. We extend this to learning systems, proving that any algorithm transforming prior P to posterior Q dissipates at least $\mathrm{E} \geq k_B T \cdot \mathrm{KL}(Q \| P)$ (Theorem 3.6).
2. **Information Theory (Section 3.5):** Rate-distortion theory bounds the minimum description length for lossy compression. We prove that achieving accuracy ϵ requires processing $I(\epsilon) = \Omega(\log(1/\epsilon))$ bits of relevant information, each costing $k_B T \ln 2$ energy (Theorem 3.12).
3. **Spectral Graph Theory (Section 9):** Attention matrices form weighted graphs whose eigenvalues govern information flow. We prove that preserving the spectral gap λ_2 ensures mixing time preservation, enabling principled sparsification (Theorem 8.5).
4. **Riemannian Geometry (Section 5):** The attention manifold's curvature controls information decay rates. Positive Ricci curvature $\kappa > 0$ causes exponential information loss $I(t) \leq I(0)e^{-\kappa t}$, while negative curvature enables sustained propagation (Theorem 5.2).
5. **Non-Equilibrium Thermodynamics (Section 6):** SGD is a discrete Langevin process with computational temperature $T_{\text{comp}} \propto \eta/B$. The second law for learning (Theorem 6.7) bounds the minimum dissipation for any training trajectory.

We further observe that the full attention graph is inherently *low-rank* and *clusterable* due to the semantic redundancy of natural language. Consequently, the dense adjacency matrix W contains statistically negligible entries that contribute to noise rather than signal.

Based on this unified framework, we introduce **Spectral Sparse Attention (SSA)**, a method rooted in Spectral Graph Theory and Randomized Numerical Linear Algebra (RandNLA). Unlike heuristic sparsity patterns (e.g., fixed windows in Longformer, hash-based routing in Reformer), SSA dynamically constructs the sparsity pattern by approximating the principal eigenspaces of the attention graph Laplacian.

Contributions. Our contributions span theory, methodology, and practice:

1. **Axiomatic Foundation (Section 3.2):** We establish three axioms—Energy Monotonicity, Learnability, and Resource Coupling—that formalize energy-efficient learning and yield the Fundamental Trade-off Theorem 3.2.
2. **Physical Lower Bounds (Section 3.4):** We derive the tightest known bounds on computational energy: $\mathrm{E} \geq k_B T \ln 2 \cdot I_{\text{processed}}$ where $I_{\text{processed}}$ is the total information processed by the algorithm.
3. **Scaling Laws from First Principles (Section 4.3):** We derive Chinchilla-style scaling laws $\mathcal{E} \sim n^{-\alpha} + p^{-\beta} + s^{-\gamma}$ from information-theoretic axioms, explaining why balanced compute-data allocation is optimal.
4. **Latency-Energy-Throughput Analysis (Section 4.2):** We prove fundamental trilemma constraints and derive optimal batch sizes for energy-efficient inference.
5. **Spectral Sparse Attention (Section 8):** We develop SSA with rigorous guarantees: $O(N^{1.5})$ complexity, spectral preservation (Theorem 9.4), and mixing time bounds (Theorem 8.5).
6. **Practical Guidelines (Section 4):** We provide concrete recommendations for energy-efficient training and inference, including optimal precision selection, sparsity patterns, and scheduling algorithms.

1.4 Theoretical Framework Overview

Figure 1 presents the logical structure of our unified theory, showing how fundamental physical laws lead to operational design principles.

2 Related Work

Efficient Attention Mechanisms. The $O(N^2)$ complexity of self-attention has motivated numerous efficient alternatives. **Sparse attention** methods include fixed patterns (Longformer [3], BigBird [32]) and learned patterns (Sparse Transformer [7]). **Linear attention** approximates softmax via kernel feature maps (Performer [8], Linear Transformer [17]), achieving $O(N)$ complexity but often sacrificing expressivity. **Hash-based routing** (Reformer [19]) uses locality-sensitive hashing to identify similar queries and keys. **Low-rank approximations** (Linformer [29], Nyströmformer [31]) exploit the empirical low-rank structure of attention matrices. Our SSA differs by providing *spectral preservation guarantees* through graph-theoretic analysis, ensuring that essential information-theoretic properties of dense attention are maintained.

Level	**Core Result**	**Practical Implication**
Level 1: Physical Laws		
Landauer Bound	$\mathrm{E} \geq k_B T \ln 2$ per bit	Ultimate efficiency limit
I/O Complexity	$Q \geq \lvert E \rvert / \log M$	Memory hierarchy design
Level 2: Information Theory		
Rate-Distortion	$\mathrm{E}(D) \geq k_B T \cdot R(D)$	Compression-energy trade-off
Info Bottleneck	$\mathrm{E}(I_0) \geq k_B T \cdot \Phi^{-1}(I_0)$	Representation learning
PAC-Bayes	$\mathcal{E} \leq \hat{\mathcal{E}} + f(\mathrm{KL}, \mathrm{E})$	Generalization bounds
Level 3: Geometry & Spectral		
Ricci Curvature	$\frac{dI}{dt} \leq -\kappa I + C$	Attention design
Spectral Gap	$\tau_{\text{mix}} \leq \frac{1}{\lambda_2} \log(1/\epsilon)$	Sparse attention bounds
Davis-Kahan	$\lVert \sin \Theta \rVert \leq \lVert E \rVert / \delta_k$	Sparsification quality
Level 4: Optimization Dynamics		
Fokker-Planck	$\partial_t \rho = \nabla \cdot (D \nabla \rho + \rho \nabla \mathcal{L})$	Training dynamics
2nd Law	$\Delta \mathcal{L} \leq -T \Delta S + W_{\text{diss}}$	Minimum dissipation
Opt. Transport	$\mathrm{E} \cdot \tau \geq W_2^2 / T_{\text{comp}}$	Speed-energy trade-off
Level 5: Design Principles		
Scaling Laws	$n^*/p^* = \alpha/\beta \cdot (B/A)^{1/(\alpha+\beta)}$	Chinchilla allocation
Trilemma	$\text{Lat} \times \text{En} \times \text{Thr}^{-1} \geq \Omega(pe_{\text{mem}})$	Inference optimization
SSA	$O(N^{1.5})$ with spectral guarantee	Long-context attention

Figure 1: Hierarchical structure of the unified energy-efficiency theory. Each level builds on the previous, connecting fundamental physics to practical algorithm design.

Memory-Efficient Implementation. FlashAttention [10] and its successor FlashAttention-2 [9] achieve exact attention with reduced memory footprint via tiling and kernel fusion, targeting the memory-bound regime. Ring Attention [23] extends this to distributed settings for near-infinite context lengths. Our approach is complementary: SSA reduces FLOPs (compute-bound regime), while FlashAttention reduces memory traffic. Combining both yields multiplicative benefits.

KV Cache Optimization. Multi-Query Attention (MQA) [26] and Grouped-Query Attention (GQA) [1] reduce KV cache size by sharing key-value heads across query heads, achieving significant memory savings during inference. These techniques are orthogonal to SSA and can be combined for additional efficiency gains.

Energy-Efficient Machine Learning. Prior work on energy efficiency has focused on **quantization** [16], **pruning** [13], and **neural architecture search** [6]. Recent post-training quantization methods such as GPTQ [12] and AWQ [22] enable aggressive 4-bit quantization with minimal quality degradation. Theoretical analyses include compute-optimal scaling laws [14] and the Chinchilla study. Our work provides a *unified theoretical foundation* connecting these approaches through thermodynamic and information-theoretic principles.

Thermodynamics of Computation. Landauer's principle [21] establishes the minimum energy for bit erasure as $k_B T \ln 2$. The physics of information was further developed by Bennett [4] who showed that logically reversible computation can in principle be performed with arbitrarily low energy dissipation. Recent work has extended thermodynamic analysis to machine learning. Wolpert [30] developed a comprehensive framework for the thermodynamics of computation, including bounds on inference and learning. Still et al. [28] connected prediction and thermodynamic efficiency through the lens of information processing. Boyd et al. [5] analyzed the thermodynamic cost of Bayesian inference. Our work builds on these foundations by: (i) deriving learning-specific bounds that incorporate task structure (Theorem 3.6), (ii) connecting thermodynamic costs to practical quantities like model size and precision, and (iii) using these principles to guide algorithm design (SSA).

Information Geometry and Learning. The geometric structure of probability distributions has deep connections to learning dynamics. Amari's information geometry [2] provides the mathematical framework relating Fisher information, natural gradient descent, and statistical manifolds. Recent work has applied these ideas to deep learning [24] and understanding attention mechanisms [18]. Our geometric analysis of attention manifolds (Section 5) extends this line of work by connecting Ricci curvature to information propagation and energy dissipation.

Complexity Comparison. Table 2 summarizes the computational complexity and key properties of various efficient attention mechanisms. SSA uniquely provides spectral preservation guarantees while achieving subquadratic complexity.

Method	**Time**	**Space**	**Exact**	**Spectral**	**Adaptive**
Dense Attention	$O(N^2d)$	$O(N^2)$	✓	✓	–
FlashAttention [10]	$O(N^2d)$	$O(N)$	✓	✓	–
Longformer [3]	$O(Nwd)$	$O(Nw)$	×	×	×
Performer [8]	$O(Nd^2)$	$O(Nd)$	×	×	–
Linformer [29]	$O(Nkd)$	$O(Nk)$	×	×	×
Reformer [19]	$O(N \log N \cdot d)$	$O(N \log N)$	×	×	✓
SSA (ours)	$O(N^{1.5}d)$	$O(N^{1.5})$	×	✓	✓

Table 2: Complexity comparison of efficient attention mechanisms. N: sequence length, d: dimension, w: window size, k: projection rank. "Exact": computes full attention. "Spectral": preserves eigenvalue structure. "Adaptive": data-dependent sparsity pattern.

2.1 Notation and Terminology

For clarity, we summarize the key notation used throughout this paper in Table 3.

Remark 2.1 (Physical vs. Computational Temperature). This paper uses two notions of temperature: (i) **Physical temperature** T (in Kelvin) appears in thermodynamic bounds like Landauer's principle, representing the thermal environment of the computing hardware. (ii) **Computational temperature** $T_{\text{comp}} \propto \eta/B$ is an *effective* temperature arising from SGD's stochastic dynamics, where η is the learning rate and B is the batch size. This analogy connects optimization theory to statistical mechanics: high T_{comp} (large η, small B) corresponds to more exploration, while low T_{comp} favors exploitation. The two temperatures are conceptually distinct but connected through the fluctuation-dissipation theorem (Section 6).

3 A Unified Mathematical Theory of Energy-Efficient AI

This section develops a general theory that abstracts away architectural details and focuses on principles that govern energy use in learning systems. We present the theory as a hierarchy: **Axioms → Fundamental Theorems → Operational Bounds → Design Principles**.

Symbol	Description
Learning System	
$\mathcal{H}$	Hypothesis space (neural network parameters)
$\mathcal{L}$	Loss functional
$\mathcal{A}$	Learning algorithm (e.g., SGD)
E	Energy functional (Joules)
$\mathcal{E}$	Error/risk function
Resources	
n	Dataset size
p	Parameter count
s	Training steps
N	Sequence length
d	Embedding dimension
b	Numerical precision (bits)
ρ	Sparsity (fraction of nonzeros)
Attention and Graphs	
Q, K, V	Query, Key, Value matrices $\in \mathbb{R}^{N \times d}$
W	Attention weight matrix $\in \mathbb{R}^{N \times N}$
$\mathcal{G}$	Attention graph
$\mathbf{L}$	Graph Laplacian (distinct from loss $\mathcal{L}$)
λ_i	Eigenvalues of Laplacian
δ_k	Spectral gap $\lambda_{k+1} - \lambda_k$
SSA Parameters	
k	Number of clusters ($\Theta(\sqrt{N})$)
s	Number of sampled inter-cluster edges ($\Theta(\sqrt{N})$)
m	Projection dimension ($O(\log N/\epsilon^2)$)
ϵ	Approximation error parameter
Thermodynamics	
k_B	Boltzmann constant (1.38×10^{-23} J/K)
T	Physical temperature (Kelvin); typically $T = 300$K
T_{comp}	Computational temperature $\propto \eta/B$ (see Remark 2.1)
$H(\cdot)$	Shannon entropy
$\mathrm{KL}(\cdot\|\cdot)$	Kullback-Leibler divergence
$I(X;Y)$	Mutual information

Table 3: Summary of notation used throughout this paper.

3.1 Thermodynamic Foundations

We begin with the physical laws that constrain all computation.

Theorem 3.1 (Landauer's Principle [21]). *Any logically irreversible computation that erases one bit of information must dissipate at least:*

$$\mathrm{E}_{\min} = k_B T \ln 2 \approx 2.9 \times 10^{-21} \text{ } J \text{ } at \text{ } T = 300K \tag{1}$$

Remark 3.1 (Gap to Landauer Limit). Modern GPUs dissipate ≈1 pJ per floating-point operation, which is $\mathbf{3 \times 10^8}$ times the Landauer limit. This gap represents the potential for improvement through reversible computing, adiabatic circuits, or thermodynamically-aware algorithms.

Definition 3.1 (Computational Entropy Production). For a computation $\mathcal{C}$ that transforms input distribution P_X to output distribution P_Y, the *computational entropy production* is:

$$\Sigma_{\mathcal{C}} = H(X|Y) + H(Y) - H(X) = I(X;Y) - H(X) + H(Y)$$

This quantifies the irreversibility of the computation.

3.2 Axiomatic Framework

We formalize the energy-efficiency problem through a set of axioms that capture the essential structure of learning under resource constraints.

Definition 3.2 (Learning System)**.** A *learning system* is a tuple $\mathcal{S} = (\mathcal{H}, \mathcal{L}, \mathcal{A}, \mathcal{M}, \mathrm{E})$ where:

- $\mathcal{H}$ is a hypothesis space (e.g., neural network parameters)
- $\mathcal{L} : \mathcal{H} \times \mathcal{D} \to \mathbb{R}_{\geq 0}$ is a loss functional
- $\mathcal{A}$ is a learning algorithm (e.g., SGD)
- $\mathcal{M}$ is a hardware model specifying computational resources
- $\mathrm{E} : \mathcal{A} \times \mathcal{M} \to \mathbb{R}_{\geq 0}$ is the energy functional

Assumption 3.1 (Axiom of Energy Monotonicity)**.** For any learning algorithm $\mathcal{A}$, the energy functional satisfies:

1. **Computation monotonicity:** $\mathrm{E}(\mathcal{A}_1 \circ \mathcal{A}_2) \geq \mathrm{E}(\mathcal{A}_1) + \mathrm{E}(\mathcal{A}_2)$
2. **Information monotonicity:** If $\mathcal{A}$ produces output with mutual information $I(X;Y)$, then $\mathrm{E}(\mathcal{A}) \geq \Omega(I(X;Y))$
3. **Irreversibility:** Any logically irreversible operation contributes $\geq k_B T \ln 2$ per erased bit

Assumption 3.2 (Axiom of Learnability)**.** For a data distribution $\mathcal{D}$ and hypothesis class $\mathcal{H}$, there exists a learning curve $\mathcal{E} : \mathbb{R}_+^k \to \mathbb{R}_+$ such that with resources $(r_1, \ldots, r_k)$ (e.g., data, compute, parameters):

$$\mathbb{E}[\mathcal{L}(h^*, \mathcal{D})] = \mathcal{E}(r_1, \ldots, r_k) + \mathcal{E}_\infty$$

where $\mathcal{E}$ is monotonically decreasing in each r_i and $\mathcal{E}_\infty$ is the irreducible error.

Assumption 3.3 (Axiom of Resource Coupling)**.** The energy functional decomposes as:

$$\mathrm{E}(r_1, \ldots, r_k) = \sum_{i=1}^{k} \alpha_i f_i(r_i) + \sum_{i<j} \beta_{ij} g_{ij}(r_i, r_j) + \mathrm{E}_0$$

where f_i, g_{ij} are nonnegative convex functions and $\alpha_i, \beta_{ij} \geq 0$ are hardware-dependent coefficients.

Theorem 3.2 (Fundamental Trade-off Theorem)**.** *Under Axioms 3.1–3.3, for any target error $\epsilon > \mathcal{E}_\infty$, the minimum energy required satisfies:*

$$\mathrm{E}^*(\epsilon) = \inf_{\{r_i : \mathcal{E}(r_1, \ldots, r_k) \leq \epsilon - \mathcal{E}_\infty\}} \mathrm{E}(r_1, \ldots, r_k)$$

Moreover, if $\mathcal{E}$ and E are smooth, the optimal allocation satisfies the marginal efficiency condition:

$$\frac{\partial \mathcal{E}/\partial r_i}{\partial \mathrm{E}/\partial r_i} = \frac{\partial \mathcal{E}/\partial r_j}{\partial \mathrm{E}/\partial r_j} \quad \forall i, j$$

Proof. The optimization problem is:

$$\min_{r_1, \ldots, r_k} \mathrm{E}(r_1, \ldots, r_k) \quad \text{s.t.} \quad \mathcal{E}(r_1, \ldots, r_k) \leq \epsilon - \mathcal{E}_\infty$$

Form the Lagrangian $\mathcal{L} = \mathrm{E} + \lambda(\mathcal{E} - \epsilon + \mathcal{E}_\infty)$. At the optimum:

$$\frac{\partial \mathrm{E}}{\partial r_i} = -\lambda \frac{\partial \mathcal{E}}{\partial r_i} \quad \Rightarrow \quad \frac{\partial \mathcal{E}/\partial r_i}{\partial \mathrm{E}/\partial r_i} = -\frac{1}{\lambda}$$

Since λ is constant across all i, the marginal efficiency condition follows. The existence of $\mathrm{E}^*(\epsilon)$ follows from the continuity of $\mathcal{E}$ and compactness of sublevel sets when E is coercive. □

Theorem 3.3 (Fundamental Energy-Accuracy Trade-off)**.** *For any learning algorithm that achieves test error ϵ on a task with information complexity I_{task}, the minimum energy satisfies:*

$$\mathrm{E}^*(\epsilon) \geq k_B T \ln 2 \cdot \left[I_{task} \cdot \log \left(\frac{1}{\epsilon - \mathcal{E}_\infty} \right) + H(model) \right] \tag{2}$$

where $H(model)$ is the description complexity of the learned model.

Furthermore, for smooth loss landscapes with condition number κ:

$$\mathrm{E}^*(\epsilon) = \Omega \left(k_B T \cdot p \cdot \kappa \cdot \log \left(\frac{\mathcal{E}_0}{\epsilon - \mathcal{E}_\infty} \right) \right) \tag{3}$$

where p is the effective parameter count and $\mathcal{E}_0$ is the initial error.

Proof. The bound follows from three information-theoretic constraints, each contributing to the total energy cost.

Step 1: Information Extraction via Rate-Distortion Theory. Consider the learning problem as a lossy compression task: the algorithm compresses the information in the training data D into a model θ. The rate-distortion function $R(\epsilon)$ gives the minimum number of bits required to encode the data-generating distribution to within distortion ϵ.

For the hypothesis class $\mathcal{H}$ and data distribution $\mathcal{D}$, define $I_{\text{task}} = I(D; Y^*)$ as the mutual information between training data and optimal predictions. The algorithm must extract at least $R(\epsilon) \geq I_{\text{task}} - I_\epsilon$ bits, where I_ϵ accounts for the allowed slack. For smooth function classes (e.g., Lipschitz functions over bounded domains), classical results [20] establish $R(\epsilon) = \Theta(d \cdot \log(1/\epsilon))$ where d is the intrinsic dimension.

Step 2: Model Storage and Description Length. The learned model θ^* must be represented in memory. By the minimum description length (MDL) principle, the optimal code length satisfies $H(\text{model}) \geq \log |\mathcal{H}_\epsilon|$ where $\mathcal{H}_\epsilon$ is the ϵ-covering number of the hypothesis class. For neural networks with p parameters at b-bit precision: $H(\text{model}) = \Theta(p \cdot b)$ bits.

Step 3: Thermodynamic Cost via Landauer's Principle. Each bit of irreversible computation—including bit erasure during gradient updates, overwriting of activations, and memory operations—costs at least $k_B T \ln 2$ energy (Theorem 3.1).

For gradient descent on a κ-conditioned landscape, convergence to ϵ-accuracy requires $\Omega(\kappa \cdot \log(\mathcal{E}_0/\epsilon))$ iterations [25]. Each iteration processes $\Theta(p)$ parameters, with gradient computation involving $\Theta(p)$ irreversible operations.

Combining the bounds: Total bits processed $\geq R(\epsilon) + H(\text{model}) + \kappa \cdot \log(1/\epsilon) \cdot p$. By Landauer:

$$\mathrm{E}^* \geq k_B T \ln 2 \cdot \left[I_{\text{task}} \cdot \log(1/\epsilon) + p \cdot b + \kappa \cdot p \cdot \log(\mathcal{E}_0/\epsilon) \right]$$

Absorbing constants and noting that $b = O(1)$ gives the stated bound. □

Remark 3.2 (Tightness and Gaps)*.* The bound in Theorem 3.3 is *order-optimal* in the sense that there exist algorithms (e.g., optimal gradient descent on quadratics) matching the $\Omega(\kappa \cdot \log(1/\epsilon))$ iteration complexity. However, the gap between Landauer's limit and practical hardware ($\approx 10^8$) means the bound is not tight in absolute terms. The theorem establishes the correct *functional form* of the energy-accuracy trade-off, which is valuable for understanding scaling behavior even when constants are loose.

Corollary 3.4 (Energy Scaling with Model Size)**.** *For a model achieving error ϵ on a task:*

$$\mathrm{E}^*(p, \epsilon) = \Theta \left(p \cdot \log(1/\epsilon) \cdot e_{flop} \right) \tag{4}$$

where the constant depends on the task complexity and optimization landscape. Doubling accuracy (halving error) increases minimum energy by ≈40% (one additional bit).

3.3 Setting, notation, and energy model

We consider supervised or self-supervised learning with dataset size n, parameter count p, training steps s, sequence length L, and per-step FLOPs $\mathrm{F}(p, L)$. A learning algorithm $\mathcal{A}$ run on hardware $\mathcal{H}$ incurs total energy

$$\mathrm{E}_{\text{total}} = \underbrace{\alpha_{\text{flop}}\,\text{FLOPs}}_{\text{arithmetic}} + \underbrace{\alpha_{\text{mem}}\,\text{Bytes}}_{\text{memory traffic}} + \underbrace{\alpha_{\text{comm}}\,\text{Words moved}}_{\text{interconnect}} + \underbrace{\alpha_{\text{ovh}}}_{\text{overheads}},$$

with technology-dependent coefficients $\alpha_{(\cdot)}$ for the target process node and accelerator. For concreteness we use the training-time proxy

$$\mathrm{E}_{\text{train}} = e_{\text{flop}}(b)\,k_{\text{flop}}\,p\,s\,g(L) + e_{\text{mem}}(b)\,k_{\text{mem}}\,p + e_{\text{comm}}\,k_{\text{comm}}\,\mathcal{B}(p, \text{HW}), \tag{5}$$

where b is numerical precision in bits, $g(L)$ captures sequence-length dependence (e.g., $g(L) = L^2$ for dense attention), and $\mathcal{B}$ the communication volume under a parallelization strategy. Similar decompositions apply at inference.

Assumptions and identifiability. Throughout, constants $k_{\text{flop}}, k_{\text{mem}}, k_{\text{comm}}$ absorb hardware- and kernel-dependent multiplicative factors. We assume: (i) $e_{\text{flop}}(b)$ and $e_{\text{mem}}(b)$ are nondecreasing in b; (ii) communication $\mathcal{B}(p, \text{HW})$ satisfies I/O lower bounds of the algorithm DAG; and (iii) learning curves (6) hold in the operating regime (power-law stationarity), with n, p, s sufficiently large to neglect finite-size effects. Identifiability is achieved by calibrating $(e_{\cdot}, k_{\cdot})$ on microbenchmarks.

Learning curves. Empirically, test loss admits power-law scaling in resources. We posit a separable model

$$\mathcal{E}(n, p, s) = \mathcal{E}_{\infty} + a\,n^{-\alpha} + b\,s^{-\beta} + c\,p^{-\gamma}, \quad \alpha, \beta, \gamma > 0, \tag{6}$$

which we use as a surrogate objective subject to an energy budget.

3.4 Fundamental lower bounds

We first state generic physical and algorithmic lower bounds, establishing the ultimate limits of energy efficiency. Note that the computational entropy production defined in Definition 3.1 quantifies irreversibility; we now derive energy bounds from this foundation.

Proposition 3.5 (Landauer-type bound)**.** *Let B be the number of logically irreversible bit erasures in an execution of $\mathcal{A}$. Then at temperature T the required energy satisfies $\mathrm{E}_{\min} \geq k_{\mathrm{B}} T \ln 2 \cdot B$.*

Remark 3.3. While digital systems operate far above this limit, Proposition 3.5 implies that any reduction in writes/erases (e.g., via activation checkpointing, sparsity, reversible layers) moves the system closer to thermodynamic efficiency.

Theorem 3.6 (Generalized Landauer Bound for Learning)**.** *Consider a learning algorithm $\mathcal{A}$ that transforms a prior P over hypotheses to a posterior Q after observing data D. The minimum energy dissipation satisfies:*

$$\mathrm{E}_{\min} \geq k_B T \ln 2 \cdot \left[\mathrm{KL}(Q\|P) + H(Q) - H(P)\right]$$

where the KL divergence term captures the information gain and the entropy difference captures the computational compression.

Proof. The learning process can be decomposed into: (i) receiving data (communication cost), (ii) updating beliefs (computation cost), and (iii) storing the posterior (memory cost). Each irreversible step contributes to entropy production.

By the second law of thermodynamics, the total entropy change satisfies:

$$\Delta S_{\text{universe}} = \Delta S_{\text{system}} + \Delta S_{\text{environment}} \geq 0$$

The system entropy change is $\Delta S_{\text{system}} = H(Q) - H(P)$. The environmental entropy change is related to heat dissipation: $\Delta S_{\text{environment}} = Q_{\text{heat}}/T$.

The information gain $I(D;\theta) = \text{KL}(Q\|P) + H(P) - H(P|D)$ must be erased from the environment (Landauer). Combining:

$$\frac{\text{E}}{T} \geq k_B \ln 2 \cdot \big[\text{KL}(Q\|P) + H(Q) - H(P)\big]$$

□

Proposition 3.7 (Communication-limited bound)**.** *In any distributed execution with per-step communication volume V and interconnect energy-per-word α_{comm}, we have $\text{E} \geq \alpha_{\text{comm}} V$. Lower bounds on V follow from I/O complexity of the computation DAG (e.g., red–blue pebble games), implying architecture-agnostic energy lower bounds.*

Theorem 3.8 (I/O Complexity Lower Bound [15])**.** *Let $\mathcal{G} = (V, E)$ be the computation DAG with $|V| = n$ operations and memory capacity M. The minimum number of I/O operations satisfies:*

$$Q \geq \frac{|E| - M \cdot \mathit{depth}(\mathcal{G})}{\log M}$$

Consequently, the minimum energy for any execution is:

$$\text{E} \geq \alpha_{IO} \cdot \frac{|E| - M \cdot \mathit{depth}(\mathcal{G})}{\log M}$$

where α_{IO} is the energy cost per I/O word.

Corollary 3.9 (Attention I/O Lower Bound)**.** *For the attention operation $\mathit{Attention}(Q, K, V) \in \mathbb{R}^{N\times d}$, any algorithm requires:*

$$Q \geq \Omega\left(\frac{N^2 d}{M}\right) \quad \textit{I/O operations}$$

implying $\text{E}_{\mathit{attn}} \geq \Omega\left(\alpha_{IO} \cdot \frac{N^2 d}{M}\right)$.

Theorem 3.10 (Attention Energy Lower Bound)**.** *For computing exact attention $Y = \text{softmax}(QK^T/\sqrt{d})V$ over N tokens with embedding dimension d:*

1. ***Information-theoretic bound:*** $\text{E} \geq k_B T \ln 2 \cdot N \cdot d \cdot \log N$ *(bits to specify output)*
2. ***Computational bound:*** $\text{E} \geq e_{\mathit{flop}} \cdot 2N^2 d$ *(irreducible FLOPs)*
3. ***I/O bound:*** $\text{E} \geq e_{IO} \cdot \frac{N^2 d}{M}$ *(memory traffic with cache size M)*

The tightest bound depends on the regime:

$$\text{E}_{\mathit{attn}} = \begin{cases} \Theta(N^2 d \cdot e_{\mathit{flop}}) & \textit{if compute-bound (large } d\textit{)} \\ \Theta(N^2/M \cdot e_{IO}) & \textit{if I/O-bound (large } N\textit{, small } M\textit{)} \end{cases} \tag{7}$$

Proof. **Information bound:** The output $Y \in \mathbb{R}^{N \times d}$ contains $N \cdot d$ floating-point numbers, each requiring $\Theta(\log N)$ bits to specify (distinguishing among N input combinations). Total: $\Theta(Nd \log N)$ bits.

Computational bound: The matrix products QK^T and $(QK^T)V$ each require $\Theta(N^2 d)$ multiply-accumulate operations. No algebraic identity reduces this for exact computation.

I/O bound: By the red-blue pebble game (Hong & Kung), any algorithm with fast memory M requires $\Omega(N^2 d/\sqrt{M})$ slow-memory accesses for matrix multiplication. For attention, the softmax prevents standard blocking, giving the stated bound. □

Corollary 3.11 (Energy Savings from Approximate Attention)**.** *Any approximate attention achieving ϵ-accuracy can reduce energy to:*

$$\mathrm{E}_{approx} \geq k_B T \ln 2 \cdot N \cdot d \cdot \log(1/\epsilon) \tag{8}$$

For $\epsilon = 0.1$: energy reduction of $\approx N/\log(1/\epsilon) \approx N/3$ compared to exact attention (when $N \gg 1$).

SSA achieves $\mathrm{E}_{SSA} = \Theta(N^{1.5} d \cdot e_{flop})$, which is optimal up to logarithmic factors for spectral-preserving approximations.

3.5 Energy–accuracy trade-offs via information theory

We link accuracy to energy through coding theorems and establish a complete information-theoretic framework.

Definition 3.3 (Learning Channel)**.** A *learning channel* is a Markov chain $X \to Z \to \hat{Y}$ where X is the input data, Z is the internal representation, and $\hat{Y}$ is the prediction. The channel is characterized by:

- **Capacity:** $C = \max_{P_X} I(X; Z)$
- **Compression rate:** $R = I(Z; X)/H(X)$
- **Relevance:** $I(Z; Y)$ for target Y

Theorem 3.12 (Information Bottleneck Energy Bound)**.** *For a learning channel $X \to Z \to \hat{Y}$ with representation complexity $I(X; Z)$ and prediction quality $I(Z; Y)$, define the Lagrangian:*

$$\mathcal{L}_{IB} = I(X; Z) - \beta I(Z; Y)$$

The minimum energy to achieve information extraction $I(Z; Y) \geq I_0$ satisfies:

$$\mathrm{E}_{\min}(I_0) \geq k_B T \ln 2 \cdot \min_{I(Z;Y) \geq I_0} I(X; Z)$$

The optimal representation lies on the information curve $I(Z; Y) = \Phi(I(X; Z))$, which is concave.

Proof. The data processing inequality gives $I(Z; Y) \leq I(X; Y)$. The representation Z can only preserve information about Y that exists in X. The encoding process requires storing at least $I(X; Z)$ bits about the input.

By Landauer's principle, encoding and subsequent erasure of $I(X; Z)$ bits costs at least $k_B T \ln 2 \cdot I(X; Z)$ energy. The optimization over valid encoders with $I(Z; Y) \geq I_0$ yields the bound.

The concavity of Φ follows from the convexity of mutual information in the conditional distribution: for representations Z_1, Z_2 achieving the same $I(X; Z)$, their mixture achieves at least the same $I(Z; Y)$. □

Theorem 3.13 (Rate–distortion energy bound). *Consider an encoder–decoder that maps inputs to a representation Z and predictions with distortion D. Let $R(D)$ be the Shannon rate–distortion function under the relevant distortion measure. Any implementation at temperature T that irreversibly erases $B \geq R(D)$ bits satisfies*

$$\mathrm{E}_{\min}(D) \;\geq\; k_{\mathrm{B}} T \ln 2 \,\cdot R(D).$$

Remark 3.4 (Examples and tightness). For a Gaussian source with squared-error distortion, $R(D) = \frac{1}{2} \log \frac{\sigma^2}{D}$. Hence $\mathrm{E}_{\min}(D) \geq \frac{1}{2} k_B T \ln 2 \log(\sigma^2/D)$. For a Bernoulli($p$) source with Hamming distortion, $R(D) = H(p) - H(D)$ for $0 \leq D \leq \min\{p, 1-p\}$. Equality is approached by implementations that minimize logically irreversible erasures (near-reversible computing), though practical systems operate far above the Landauer limit.

Proof sketch. Achieving distortion D requires communicating at least $R(D)$ bits about the source. Each irreversibly erased bit dissipates $k_{\mathrm{B}} T \ln 2$ energy by Landauer; hence the bound. □

Theorem 3.14 (Channel Capacity–Energy Trade-off). *Consider a communication channel with capacity C bits per transmission. The minimum energy per bit to achieve reliable communication at rate $R < C$ satisfies:*

$$\mathrm{E}_{bit} \geq \frac{N_0 \ln 2}{1 - R/C} \cdot R$$

where N_0 is the noise spectral density. At capacity ($R \to C$), the energy per bit diverges.

Theorem 3.15 (Energy-aware PAC-Bayes). *Let Q be the posterior over hypotheses after training and P a prior. With probability $1 - \delta$ over samples of size n,*

$$\mathcal{E}(h) \;\leq\; \hat{\mathcal{E}}(h) \;+\; \sqrt{\frac{\mathrm{KL}(Q \,\|\, P) + \log \frac{2\sqrt{n}}{\delta}}{2(n-1)}} \;+\; \lambda \, \frac{\mathrm{E}_{\mathrm{train}}}{n},$$

for all $h \sim Q$ and any $\lambda > 0$. Thus minimizing empirical loss with an energy penalty controls generalization.

Corollary 3.16 (Energy-Complexity Trade-off). *The description length of a hypothesis h satisfies $DL(h) \geq \mathrm{KL}(Q_h \| P)$. Combined with Theorem 3.15, this gives:*

$$\mathcal{E}(h) \leq \hat{\mathcal{E}}(h) + O\left(\sqrt{\frac{DL(h)}{n}}\right) + O\left(\frac{\mathrm{E}}{n}\right)$$

implying a three-way trade-off between empirical error, model complexity, and energy.

3.6 Connecting Theory to Large Model Training

We now explicitly connect the abstract information-theoretic bounds to practical quantities in large model training.

Theorem 3.17 (Training Energy from Information Theory). *For training a model with p parameters on n data points to achieve test loss $\mathcal{L}$, the minimum energy satisfies:*

$$\mathrm{E}_{train} \geq k_B T \ln 2 \cdot \underbrace{n \cdot H(Y|X)}_{\text{label entropy}} + k_B T \ln 2 \cdot \underbrace{p \cdot b}_{\text{model storage}} + k_B T \ln 2 \cdot \underbrace{I(D;\theta)}_{\text{information extraction}} \tag{9}$$

where $H(Y|X)$ is the conditional entropy of labels given inputs, b is precision, and $I(D;\theta)$ is the mutual information between data and learned parameters.

Proof. Training involves three irreversible information processes:

1. **Data streaming:** Processing n data points with $H(Y|X)$ bits of label information each
2. **Model materialization:** Storing $p \cdot b$ bits of model parameters
3. **Learning:** Extracting $I(D;\theta)$ bits of task-relevant information

By Landauer, each bit costs at least $k_B T \ln 2$, giving the bound. □

Example 3.1 (Information Budget for GPT-3). For GPT-3 (175B parameters, 300B tokens):

- Label entropy: 300B $\times$ 16 bits/token $= 4.8 \times 10^{12}$ bits
- Model storage: 175B $\times$ 16 bits $= 2.8 \times 10^{12}$ bits
- Information extraction: $\approx I(D;\theta) \approx 10^{11}$ bits (estimated from validation loss improvement)

Total information: $\approx 7.7 \times 10^{12}$ bits

At Landauer limit: $\mathrm{E}_{\min} = 7.7 \times 10^{12} \times 2.9 \times 10^{-21} = 2.2 \times 10^{-8}$ Joules

Actual training energy: ≈ 1300 MWh $= 4.7 \times 10^{12}$ Joules

Efficiency gap: $\frac{4.7 \times 10^{12}}{2.2 \times 10^{-8}} \approx 2 \times 10^{20}$

This enormous gap (20 orders of magnitude) represents the combined inefficiency of:

- Digital logic ($\sim 10^8$ above Landauer)
- Memory hierarchy ($\sim 10^3$)
- Algorithmic overhead ($\sim 10^4$)
- Parallelization inefficiency ($\sim 10^2$)
- Cooling and infrastructure ($\sim 10^3$)

Theorem 3.18 (Inference Energy Bound). *For autoregressive inference generating T tokens from a model with p parameters:*

$$\mathrm{E}_{inference} \geq k_B T \ln 2 \cdot T \cdot \left[H(\textit{next token}) + \log p\right] \tag{10}$$

where $H(\textit{next token}) \approx$ perplexity in bits.

For practical systems:

$$\mathrm{E}_{inference} \approx e_{mem} \cdot p \cdot T + e_{flop} \cdot 2p \cdot T + e_{cache} \cdot 2Nd \cdot T \tag{11}$$

where the first term dominates (memory-bound regime) for small batch sizes.

Corollary 3.19 (Energy per Token vs. Model Quality). *For a model achieving perplexity PPL (lower is better):*

$$\frac{\mathrm{E}_{per\text{-}token}}{\textit{information output}} = \frac{\mathrm{E}_{per\text{-}token}}{\log PPL} \geq k_B T \ln 2 \tag{12}$$

Reducing perplexity by half (PPL → PPL/2) increases energy efficiency by $\log_2(2)/\log_2(PPL)$ *per useful bit of output.*

3.7 Optimal allocation under an energy budget

We now optimize (6) subject to (5) with a budget $\mathrm{E}_{\max}$.

Theorem 3.20 (Closed-form scaling under separable power laws). *Assume $\mathcal{E}(n,p,s)$ as in* (6) *and $\mathrm{E} = a_c\, p\, s + a_d\, n + a_m\, p$ (absorbing constants). The Lagrangian optimum satisfies marginal efficiency equalization:*

$$\alpha\, a\, n^{-\alpha-1}\big/a_d \;=\; \beta\, b\, s^{-\beta-1}\big/a_c p \;=\; \gamma\, c\, p^{-\gamma-1}\big/(a_c s + a_m),$$

yielding scaling laws $n^\star \propto \mathrm{E}_{\max}^{\frac{1}{\alpha+1}}$, $s^\star \propto \mathrm{E}_{\max}^{\frac{1}{\beta+1}}$, and $p^\star \propto \mathrm{E}_{\max}^{\frac{1}{\gamma+1}}$ up to hardware-dependent coefficients.

Remark 3.5. Theorem 3.20 recovers "balanced" allocation rules: energy is best spent where the marginal error reduction per Joule is largest, explaining observed compute–data trade-offs.

3.8 Precision, sparsity, and optimality

Let b be weight/activation precision and ρ the activation sparsity (fraction of nonzeros).

Proposition 3.21 (Bit-precision trade-off)**.** *Suppose quantization error contributes variance $\sigma_q^2 \propto 2^{-2b}$ while per-FLOP energy $e_{\text{flop}}(b)$ grows superlinearly in b. Then for a target excess risk Δ, the optimal b^* minimizes $e_{\text{flop}}(b)$ subject to $\sigma_q^2 \le \Delta$, yielding $b^* \asymp \frac{1}{2}\log_2 \frac{\kappa}{\Delta}$ for problem-dependent κ.*

Theorem 3.22 (Optimal Quantization Strategy)**.** *For a neural network with weights $\{w_i\}_{i=1}^p$ and per-layer sensitivities $\{s_i\}_{i=1}^L$, the energy-optimal bit allocation $\{b_i\}$ under total bit budget B_{total} satisfies:*

$$b_i^* = \bar{b} + \frac{1}{2}\log_2\left(\frac{s_i}{\bar{s}}\right)$$

where $\bar{b} = B_{total}/L$ and $\bar{s} = \left(\prod_{i=1}^L s_i\right)^{1/L}$ is the geometric mean sensitivity.

Proof. The quantization error for layer i with precision b_i is $\epsilon_i \propto s_i \cdot 2^{-b_i}$. The total error $\epsilon_{\text{total}} = \sum_i \epsilon_i$ should be minimized under the constraint $\sum_i b_i = B_{\text{total}}$.

Using Lagrange multipliers:

$$\frac{\partial}{\partial b_i}\left[\sum_j s_j 2^{-b_j}\right] = \lambda \quad \Rightarrow \quad s_i \ln(2) \cdot 2^{-b_i} = \lambda$$

Solving: $b_i = \log_2(s_i \ln 2) - \log_2(\lambda)$. Substituting into the constraint and solving for λ yields the stated result. □

Proposition 3.23 (Sparsity–energy Pareto frontier)**.** *If FLOPs scale as ρ and accuracy degrades as $\Delta(\rho) \sim c\,\rho^{-\eta}$ for $\rho \in (0,1]$, then Pareto-optimal points satisfy $\partial\Delta/\partial\rho = -\lambda\,\partial \mathrm{E}/\partial\rho$ for some $\lambda \ge 0$. In architectures where structured sparsity preserves spectral gaps (e.g., SSA), η can be large, shifting the frontier toward lower energy.*

Theorem 3.24 (Structured vs. Unstructured Sparsity)**.** *Let $W \in \mathbb{R}^{m\times n}$ be a weight matrix. Define:*

- ***Unstructured sparsity:*** $\|W\|_0 \le s$ *(arbitrary pattern)*
- ***Block sparsity:*** *W has at most b nonzero $k \times k$ blocks*
- ***Low-rank:*** $\text{rank}(W) \le r$

The energy-approximation trade-offs satisfy:

$$\begin{aligned} \mathrm{E}_{unstructured}(s) &= \Theta(s) \cdot e_{flop} + \Theta(s) \cdot e_{mem} \\ \mathrm{E}_{block}(b) &= \Theta(bk^2) \cdot e_{flop} + \Theta(b) \cdot e_{mem} \\ \mathrm{E}_{low\text{-}rank}(r) &= \Theta((m+n)r) \cdot e_{flop} + \Theta(r) \cdot e_{mem} \end{aligned}$$

For the same approximation error ϵ, the optimal structure depends on the spectrum of W: low-rank is superior when eigenvalues decay rapidly; block sparsity is superior for locally clustered structure.

3.9 Energy-aware scheduling and control

We present a practical controller that adapts batch size, sequence length, precision, and sparsity to track a target energy rate.

Algorithm 1 Energy-Aware Training Scheduler

```
Input: budget $\mathrm{E}_{\max}$, horizon $H$, initial $(b, \rho, L, \text{batch})$
for $t = 1, \dots, H$ do
    Measure $\hat{\mathrm{E}}_t$ per step; estimate marginal utility $\partial\hat{\mathcal{E}}/\partial(b, \rho, L, \text{batch})$
    Update controls by projected gradient to maximize error reduction per Joule
    Enforce constraints (throughput, memory) and (5)
end for
```

Connection to SSA. In attention layers, $g(L)$ in (5) can be reduced from $\Theta(L^2)$ to $\tilde{\Theta}(L^{1.5})$ via SSA while controlling $\Delta(\rho)$ through spectral guarantees (Theorems 8.5 and 9.4), shifting the Pareto frontier.

4 Practical Implications for Large AI Models

This section bridges the abstract theory to concrete implications for training and deploying large AI models, providing quantitative predictions validated against real-world systems.

4.1 Energy Accounting for Frontier Models

We decompose the total energy budget of a large model into its fundamental components.

Theorem 4.1 (Energy Decomposition for Transformer Training)**.** *For a Transformer with L layers, hidden dimension d, H attention heads, sequence length N, trained for S steps on n tokens with batch size B, the total training energy decomposes as:*

$$\mathrm{E}_{train} = \underbrace{e_{flop} \cdot 6pS}_{Forward/Backward} + \underbrace{e_{attn} \cdot 4LHN^2dS/B}_{Attention} + \underbrace{e_{mem} \cdot p \cdot \lceil S/C \rceil}_{Checkpointing} + \underbrace{e_{comm} \cdot V_{allreduce}}_{Communication} \tag{13}$$

where $p = 12Ld^2$ is the dense parameter count, C is the checkpoint interval, and $V_{allreduce}$ is the gradient synchronization volume.

Example 4.1 (GPT-3 175B Energy Budget)*.* For GPT-3 with $L = 96$, $d = 12288$, $H = 96$, $N = 2048$, trained for 300B tokens:

$$\begin{aligned}
\text{Forward/Backward FLOPs:} \quad & 6 \times 175\text{B} \times 300\text{B} = 3.15 \times 10^{23} \\
\text{Attention FLOPs:} \quad & 4 \times 96 \times 96 \times 2048^2 \times 12288 \times \frac{300\text{B}}{2048} = 9.2 \times 10^{22} \\
\text{Attention fraction:} \quad & \frac{9.2 \times 10^{22}}{3.15 \times 10^{23}} \approx 29\%
\end{aligned}$$

At 32K context length, attention would consume **87%** of total compute—motivating our focus on efficient attention.

4.2 Latency-Energy-Throughput Trilemma

For inference systems, three metrics are in fundamental tension: latency (time per token), energy (Joules per token), and throughput (tokens per second per GPU).

Theorem 4.2 (Inference Trilemma)**.** *For autoregressive inference of a model with p parameters and d-dimensional KV cache, any implementation satisfies:*

$$\textit{Latency} \times \textit{Energy}_{\textit{per-token}} \times \textit{Throughput}^{-1} \geq \Omega\left(\frac{p \cdot e_{mem}}{B_{mem}}\right) \tag{14}$$

where B_{mem} is memory bandwidth and e_{mem} is energy per byte transferred.

The optimal operating point depends on the use case:

- ***Interactive (low latency):*** *Small batch, high energy-per-token*
- ***Batch processing (high throughput):*** *Large batch, memory-limited*
- ***Energy-optimal:*** *Batch size $B^* = \sqrt{p/(N \cdot d)}$, balancing compute and memory*

Proof. Autoregressive decoding is memory-bound: each token requires loading p parameters from HBM. The minimum time per token is $\tau_{\min} = p/B_{\text{mem}}$. Energy per token is at least $e_{\text{mem}} \cdot p$ (parameter loading) plus KV cache access $e_{\text{mem}} \cdot 2Nd$ per token.

For batch size B:

- Latency: $\tau(B) = \max\left(\frac{p}{B_{\text{mem}}}, \frac{2pB}{F_{\text{peak}}}\right)$ where F_{peak} is compute throughput
- Energy: $\mathrm{E}(B) = e_{\text{mem}} \cdot p + e_{\text{flop}} \cdot 2p + e_{\text{cache}} \cdot 2NdB$
- Throughput: $T(B) = B/\tau(B)$

The product $\tau \cdot \mathrm{E} \cdot T^{-1} = \mathrm{E}/B$ is minimized when compute and memory costs balance, yielding $B^* = \sqrt{p/(Nd)}$. □

Remark 4.1 (Memory Constraints on Batch Size)*.* The theoretical optimal B^* may exceed available GPU memory. In practice, the achievable batch size is constrained by $B_{\max} = \lfloor (M_{\text{GPU}} - M_{\text{model}} - M_{\text{overhead}})/(2Nd \cdot b_{\text{KV}}) \rfloor$, where M_{GPU} is total GPU memory, M_{model} is model weight memory, M_{overhead} accounts for activations and workspace, and b_{KV} is bytes per KV cache element. For large models like GPT-4, the theoretical $B^* \approx 671$ at 2K context far exceeds practical limits of $B_{\max} \approx 8$–32 on current hardware. The actual operating point should be $\min(B^*, B_{\max})$.

Model	p	B^* **(2K ctx)**	B^* **(32K ctx)**	**Energy/tok (mJ)**	**Optimal tokens/J**
LLaMA-7B	7B	42	10	1.2	833
LLaMA-70B	70B	132	33	12	83
GPT-3 175B	175B	209	52	30	33
GPT-4 (est.)	1.8T	671	168	310	3.2

Table 4: Optimal batch sizes and energy efficiency for various models on H100 GPU ($B_{\text{mem}} = 3.35$ TB/s, $e_{\text{mem}} = 20$ pJ/byte, $d = d_{\text{model}}/H$). Note: B^* values are theoretical optima; practical batch sizes are often limited by GPU memory constraints.

4.3 Energy-Optimal Scaling Laws

We derive compute-optimal scaling from energy minimization principles.

Theorem 4.3 (Energy-Optimal Scaling Law)**.** *Under the power-law loss model $\mathcal{E}(n,p) = \mathcal{E}_\infty + An^{-\alpha} + Bp^{-\beta}$ and energy model $\mathrm{E} = e_{flop} \cdot 6np$, the energy-optimal allocation satisfies:*

$$\frac{n^*}{p^*} = \frac{\alpha}{\beta} \cdot \frac{B}{A}^{\frac{1}{\alpha+\beta}} \tag{15}$$

With empirical values $\alpha \approx 0.34$, $\beta \approx 0.28$ (Hoffmann et al.), this gives:

$$n^* \approx 20 \cdot p^* \tag{16}$$

i.e., the optimal token count scales as 20× the parameter count, matching the Chinchilla finding.

Proof. We minimize $\mathcal{E}(n, p)$ subject to $\mathrm{E}(n, p) = E_{\text{budget}}$, where $\mathrm{E} = c \cdot n \cdot p$ (ignoring constants).

Lagrangian: $\mathcal{L} = An^{-\alpha} + Bp^{-\beta} + \lambda(cnp - E)$

First-order conditions:

$$\frac{\partial \mathcal{L}}{\partial n} = -A\alpha n^{-\alpha-1} + \lambda cp = 0$$
$$\frac{\partial \mathcal{L}}{\partial p} = -B\beta p^{-\beta-1} + \lambda cn = 0$$

Dividing: $\frac{A\alpha n^{-\alpha-1}}{B\beta p^{-\beta-1}} = \frac{p}{n}$

Solving: $n^{\alpha+1}/p^{\beta+1} = (A\alpha)/(B\beta) \cdot (n/p)$

This gives $n/p = \left(\frac{A\alpha}{B\beta}\right)^{1/(\alpha+\beta)}$, independent of the budget E. □

Corollary 4.4 (Iso-Loss Scaling). *To achieve a target loss $\mathcal{E}^*$, the minimum energy scales as:*

$$\mathrm{E}^*(\mathcal{E}^*) = \Theta\left((\mathcal{E}^* - \mathcal{E}_\infty)^{-(\alpha+\beta)/\alpha\beta}\right) \tag{17}$$

This implies exponentially increasing energy cost for linear loss improvements.

Example 4.2 (Energy to Achieve GPT-4 Quality). Assuming GPT-4 achieves $\mathcal{E}^* \approx 0.05$ on a benchmark and $\mathcal{E}_\infty \approx 0.02$:

- Reducing error by 10% (to 0.045) requires ≈1.8× more energy
- Reducing error by 50% (to 0.035) requires ≈8× more energy
- Halving the gap to $\mathcal{E}_\infty$ (to 0.035) requires ≈16× more energy

This underscores the importance of algorithmic efficiency improvements over brute-force scaling.

4.4 Quantization and Mixed-Precision Energy Trade-offs

Precision directly impacts both computation and memory energy.

Theorem 4.5 (Precision-Energy-Accuracy Trade-off). *For a neural network quantized to b bits with quantization noise $\sigma_q^2 = \frac{\Delta^2}{12}$ where $\Delta = 2^{-b}$ is the step size:*

1. ***Compute energy:*** *$e_{flop}(b) \propto b^{1.5}$ for digital circuits, $\propto b^2$ for analog*
2. ***Memory energy:*** *$e_{mem}(b) \propto b$ (bandwidth-limited)*
3. ***Accuracy degradation:*** *$\Delta\mathcal{E} \approx c_{sens} \cdot 2^{-2b}$ for smooth loss landscapes*

The energy-optimal precision satisfies:

$$b^* = \frac{1}{2}\log_2\left(\frac{c_{sens}}{\Delta\mathcal{E}_{tol}}\right) + O(1) \tag{18}$$

For typical Transformers, $b^* \approx 4$ bits for inference, $b^* \approx 8$ bits for training.

Precision	$e_{\textbf{flop}}$ (pJ)	$e_{\textbf{mem}}$ (pJ/bit)	Relative Energy	Typical ΔErr
FP32	0.9	0.5	1.0×	0%
FP16	0.4	0.25	0.45×	<0.1%
INT8	0.2	0.125	0.22×	<1%
INT4	0.1	0.0625	0.11×	2–5%

Table 5: Energy cost and accuracy trade-offs for different precisions (7nm process).

4.5 Memory-Compute Trade-offs in Long-Context Models

Long-context models face a fundamental memory-compute trade-off.

Theorem 4.6 (Memory-Energy Trade-off for Attention)**.** *For attention over N tokens with KV cache in HBM of capacity M:*

1. ***Dense attention:*** $\mathrm{E}_{dense} = e_{flop} \cdot 2N^2 d + e_{mem} \cdot N^2$ *(if $N^2 > M$, requires recomputation)*
2. ***FlashAttention:*** $\mathrm{E}_{flash} = e_{flop} \cdot 2N^2 d + e_{mem} \cdot \frac{N^2 d}{M_{SRAM}}$ *(reduced HBM traffic)*
3. ***SSA:*** $\mathrm{E}_{SSA} = e_{flop} \cdot 2N^{1.5} d + e_{mem} \cdot N^{1.5}$

For $N > M^{1/2}$, SSA achieves energy reduction factor:

$$\frac{\mathrm{E}_{SSA}}{\mathrm{E}_{dense}} \leq O\left(N^{-0.5}\right) \tag{19}$$

Example 4.3 (Energy Savings at 128K Context)*.* For a 70B model at 128K context:

- Dense attention: $2 \times 128K^2 \times 8192 \times 80 = 2.1 \times 10^{17}$ FLOPs per layer
- SSA ($N^{1.5}$): $2 \times 128K^{1.5} \times 8192 \times 80 = 6.0 \times 10^{14}$ FLOPs per layer
- Energy reduction: **350**× per attention layer
- Total model energy reduction: ≈47% (attention is 40% of compute at this length)

4.6 Inference Serving: Energy-Optimal Batching

Production inference systems must balance latency SLAs with energy efficiency.

Theorem 4.7 (Energy-Optimal Continuous Batching)**.** *For a serving system with arrival rate λ (requests/second), SLA latency $\tau_{\max}$, and model parameters p:*

The energy-optimal batching strategy uses dynamic batch size:

$$B^*(t) = \min\left(B_{\max}, \lfloor \lambda \cdot (\tau_{\max} - \tau_{compute}(B)) \rfloor\right) \tag{20}$$

where $\tau_{compute}(B)$ is the compute time per batch.

The expected energy per request is:

$$\mathbb{E}[\mathrm{E}_{req}] = \frac{e_{static} \cdot \tau_{\max}}{B^*} + e_{dynamic}(B^*) \tag{21}$$

minimized at $B^* = \sqrt{e_{static} \cdot \tau_{\max} / e_{marginal}}$.

4.7 Hardware-Algorithm Co-optimization

The theory suggests several hardware-algorithm co-optimization opportunities:

Proposition 4.8 (Optimal Memory Hierarchy)**.** *For attention computation, the optimal SRAM size satisfies:*

$$M^*_{SRAM} = \Theta(\sqrt{N \cdot d}) \tag{22}$$

balancing tile reuse against on-chip area cost. For $N = 32K$, $d = 128$: $M^*_{SRAM} \approx 2$ MB, matching modern GPU L2 cache sizes.

Proposition 4.9 (Sparsity-Aware Accelerators)**.** *For SSA-style sparse attention with density $\rho = N^{-0.5}$:*

1. ***Index overhead:*** *$O(\rho \cdot N^2 \cdot \log N)$ bits for sparse indices*
2. ***Compute savings:*** *$O((1-\rho) \cdot N^2)$ FLOPs saved*
3. ***Break-even:*** *Sparsity beneficial when $\rho < 1 - \frac{c_{idx} \cdot \log N}{c_{flop} \cdot d}$*

For $d = 128$, $c_{idx}/c_{flop} \approx 0.1$: break-even at $\rho \approx 0.85$, satisfied by SSA at $N > 100$.

5 Riemannian Geometry of Attention Manifolds

This section develops a differential geometric framework for understanding attention mechanisms, revealing deep connections between information flow, curvature, and energy.

5.1 The Attention Manifold

Definition 5.1 (Token Manifold)**.** Let $X = \{x_1, \dots, x_N\} \subset \mathbb{R}^d$ be a sequence of token embeddings. The *token manifold* $\mathcal{M}_X$ is the Riemannian submanifold of $\mathbb{R}^d$ defined by the convex hull of tokens equipped with the Fisher-Rao metric.

Definition 5.2 (Attention Metric Tensor)**.** For query q and key distribution over tokens, define the metric tensor at point $p \in \mathcal{M}_X$:

$$g_{ij}(p) = \mathbb{E}_{k \sim P(\cdot|p)} \left[\frac{\partial \log P(k|p)}{\partial p_i} \frac{\partial \log P(k|p)}{\partial p_j} \right]$$

This is the Fisher information matrix of the attention distribution, making $(\mathcal{M}_X, g)$ an information-geometric manifold.

Proposition 5.1 (Softmax Attention Metric)**.** *For softmax attention $P(k_j|q) = \frac{\exp(q^T k_j/\sqrt{d})}{\sum_l \exp(q^T k_l/\sqrt{d})}$, the metric tensor is:*

$$g_{ij}(q) = \frac{1}{d} \left[\mathbb{E}[k_i k_j] - \mathbb{E}[k_i]\mathbb{E}[k_j] \right] = \frac{1}{d} Cov_P(k_i, k_j)$$

where expectations are under the attention distribution.

Proof. The log-probability is $\log P(k|q) = \frac{q^T k}{\sqrt{d}} - \log Z(q)$ where $Z(q) = \sum_l \exp(q^T k_l/\sqrt{d})$.

$$\frac{\partial \log P(k|q)}{\partial q_i} = \frac{k_i}{\sqrt{d}} - \frac{1}{Z}\frac{\partial Z}{\partial q_i} = \frac{k_i}{\sqrt{d}} - \frac{\mathbb{E}[k_i]}{\sqrt{d}}$$

Thus:

$$g_{ij} = \mathbb{E}\left[\frac{(k_i - \mathbb{E}[k_i])(k_j - \mathbb{E}[k_j])}{d} \right] = \frac{\text{Cov}(k_i, k_j)}{d}$$

□

5.2 Curvature and Information Flow

Definition 5.3 (Attention Ricci Curvature)**.** The Ricci curvature of the attention manifold in direction v is:

$$\mathrm{Ric}(v, v) = \sum_{j=1}^{d} R(v, e_j, v, e_j)$$

where R is the Riemann curvature tensor and $\{e_j\}$ is an orthonormal frame.

Theorem 5.2 (Curvature-Information Trade-off)**.** *Let $\mathcal{M}$ be the attention manifold with Ricci curvature bounded below by κ. The mutual information flow rate through attention satisfies:*

$$\frac{dI(X; Z)}{dt} \leq -\kappa \cdot I(X; Z) + C_{source}$$

where C_{source} is the information injection rate from the input. Positive curvature ($\kappa > 0$) causes exponential information decay; negative curvature allows sustained information propagation.

Proof. The evolution of probability density ρ on $\mathcal{M}$ under attention-guided diffusion satisfies:

$$\frac{\partial \rho}{\partial t} = \Delta_g \rho + \nabla \cdot (\rho \nabla \Phi)$$

where Δ_g is the Laplace-Beltrami operator and Φ is the attention potential.

By the Bakry-Émery criterion, if $\mathrm{Ric} + \mathrm{Hess}(\Phi) \geq \kappa$, then the log-Sobolev inequality holds:

$$\mathrm{Ent}_\pi(\rho) \leq \frac{1}{2\kappa} I_\pi(\rho)$$

where Ent is relative entropy and I is Fisher information. This implies:

$$\frac{d}{dt}\mathrm{Ent}_\pi(\rho_t) \leq -2\kappa \cdot \mathrm{Ent}_\pi(\rho_t)$$

Relating entropy to mutual information gives the stated bound. □

Corollary 5.3 (Optimal Attention Geometry)**.** *The energy-optimal attention mechanism corresponds to a manifold with:*

1. ***Nearly flat regions** (low $|\kappa|$) for stable information storage*
2. ***Negative curvature channels** for efficient information transport*
3. ***Positive curvature boundaries** for information containment*

SSA achieves this by preserving cluster structure (flat within clusters) while sparsifying inter-cluster connections (controlled curvature).

5.3 Geodesic Attention Paths

Definition 5.4 (Attention Geodesic)**.** A curve $\gamma : [0, 1] \to \mathcal{M}_X$ is an *attention geodesic* if it minimizes the energy functional:

$$E[\gamma] = \int_0^1 g_{\gamma(t)}(\dot{\gamma}(t), \dot{\gamma}(t))\, dt$$

subject to $\gamma(0) = x_i$ and $\gamma(1) = x_j$ for tokens x_i, x_j.

Theorem 5.4 (Geodesic Distance and Attention Weights). *Let $d_g(x_i, x_j)$ be the geodesic distance on the attention manifold. For well-separated clusters with cluster centers $\{c_1, \ldots, c_k\}$, the attention weight satisfies:*

$$W_{ij} = \exp\left(-\frac{d_g(x_i, x_j)^2}{2\sigma^2}\right) \cdot (1 + O(\epsilon_{cluster}))$$

where $\sigma = \sqrt{d}$ and $\epsilon_{cluster}$ is the clustering approximation error.

Proof. For Gaussian-like attention kernels, $W_{ij} \propto \exp(-\|q_i - k_j\|^2/2d)$. The Euclidean distance in embedding space approximates the geodesic distance when:

1. The manifold is locally flat (within clusters)
2. The metric tensor is approximately constant

Under the clustered structure assumption, $g_{ij}(p) \approx g_{ij}(c_k)$ for p in cluster k. The correction term bounds the deviation from true geodesic distance. □

Proposition 5.5 (Sparse Geodesic Approximation). *Let $\mathcal{G}_{sparse}$ be a sparse graph with edges only within clusters and between cluster centers. The shortest path distance $d_{\mathcal{G}}(i, j)$ satisfies:*

$$d_g(x_i, x_j) \leq d_{\mathcal{G}}(x_i, x_j) \leq d_g(x_i, x_j) + 2 \cdot diam(cluster)$$

where $diam(cluster)$ is the maximum cluster diameter.

5.4 Heat Kernel and Spectral Geometry

Definition 5.5 (Attention Heat Kernel). The heat kernel $K_t(x, y)$ on the attention manifold satisfies:

$$\frac{\partial K_t}{\partial t} = \Delta_g K_t, \quad K_0(x, y) = \delta(x - y)$$

The multi-layer attention output approximates heat kernel convolution at time $t \propto L$ (number of layers).

Theorem 5.6 (Spectral Decomposition of Attention). *Let $\{\phi_n, \lambda_n\}$ be the eigenfunctions and eigenvalues of $-\Delta_g$ on $\mathcal{M}_X$. The attention operation after L layers approximates:*

$$Attention^L(f)(x) \approx \sum_{n=0}^{\infty} e^{-\lambda_n \tau L} \langle f, \phi_n \rangle \phi_n(x)$$

where τ is an effective time constant per layer. High-frequency modes (λ_n large) are exponentially suppressed, acting as a low-pass filter.

Corollary 5.7 (Energy-Frequency Trade-off). *Preserving the first k spectral modes requires $O(k)$ eigenvalue computations and $O(Nk)$ storage. The energy cost scales as:*

$$\mathrm{E}_{spectral}(k) = \Theta(k \cdot N \cdot e_{flop}) + \Theta(kd \cdot e_{mem})$$

Truncating to $k = O(\sqrt{N})$ modes achieves $O(N^{1.5})$ energy while preserving essential spectral information.

6 Energy-Constrained Optimization Dynamics

To make the theory actionable for AI practice, we must understand how energy constraints influence the training dynamics itself. We model Stochastic Gradient Descent (SGD) as a discretized Langevin diffusion process and analyze the thermodynamic cost of optimization.

6.1 Fokker-Planck Description of Learning

Definition 6.1 (Parameter Distribution Evolution)**.** Let $\rho(\theta, t)$ be the probability density over parameter space Θ at time t. The evolution under SGD is described by the Fokker-Planck equation:

$$\frac{\partial \rho}{\partial t} = \nabla \cdot (D(\theta)\nabla\rho + \rho\nabla\mathcal{L}(\theta))$$

where $D(\theta)$ is the diffusion tensor arising from gradient noise.

Theorem 6.1 (Entropy Production in Learning)**.** *The rate of entropy production during SGD training is:*

$$\dot{\Sigma} = \int_\Theta \frac{\|J(\theta)\|^2}{\rho(\theta)D(\theta)} d\theta \geq 0$$

where $J(\theta) = -D(\theta)\nabla\rho - \rho\nabla\mathcal{L}$ is the probability current. This entropy is dissipated as heat, contributing to energy consumption.

Proof. The entropy of ρ is $S[\rho] = -\int \rho \log\rho \, d\theta$. Taking the time derivative:

$$\dot{S} = -\int \frac{\partial \rho}{\partial t}(1 + \log\rho)d\theta = \int \nabla \cdot J \cdot \log\rho \, d\theta$$

Integration by parts and using the Fokker-Planck equation:

$$\dot{S} = -\int \frac{J \cdot \nabla\rho}{\rho} d\theta = \int \frac{\|J\|^2}{\rho D} d\theta - \int \frac{J \cdot \nabla\mathcal{L}}{D} d\theta$$

The first term is always non-negative (entropy production); the second relates to energy extraction from the loss landscape. □

6.2 Langevin Dynamics and Free Energy

The continuous-time limit of SGD with learning rate η and batch size B is given by the Stochastic Differential Equation (SDE):

$$d\theta_t = -\nabla\mathcal{L}(\theta_t)dt + \sqrt{2D(\theta_t)}dW_t \tag{23}$$

where $D(\theta_t) \approx \frac{\eta}{2B}\Sigma(\theta_t)$ is the diffusion matrix arising from gradient noise covariance Σ. We associate a *computational temperature* $T_{comp} \propto \frac{\eta}{B}$.

Theorem 6.2 (Fluctuation-Dissipation for SGD)**.** *For SGD at equilibrium with the loss landscape, the fluctuation-dissipation relation holds:*

$$D(\theta) = T_{comp} \cdot \chi(\theta)$$

where $\chi(\theta) = (\nabla^2\mathcal{L}(\theta))^{-1}$ is the susceptibility (inverse Hessian). This implies:

1. *High curvature regions (large Hessian eigenvalues) have suppressed fluctuations*
2. *Flat regions allow larger exploration with the same energy*

Theorem 6.3 (Thermodynamic Cost of Learning)**.** *Let ρ_t be the law of θ_t and let the target Gibbs posterior be $\pi(\theta) \propto e^{-\beta\mathcal{L}(\theta)}$. Define the information distance $I(t) = \mathrm{KL}(\rho_t \,\|\, \pi)$. Under Langevin dynamics with state-dependent diffusion $D(\theta)$ and with per-step energy expenditure e_{step} dominated by gradient computations, there exists a problem-dependent constant $\eta_{\text{eff}} > 0$ such that for any horizon $[t_0, t_1]$,*

$$\int_{t_0}^{t_1} \mathsf{power}(t)\, dt \;=\; \Delta\mathrm{E} \;\geq\; \frac{1}{\eta_{\text{eff}}} \big(I(t_0) - I(t_1)\big).$$

Equivalently, the instantaneous dissipation obeys $\mathsf{power}(t) \geq \frac{1}{\eta_{\text{eff}}} \big(-\dot{I}(t)\big)$.

Proof sketch. For overdamped Langevin, the evolution of $I(t)$ satisfies the de Bruijn identity and entropy dissipation: $-\dot{I}(t) = \mathcal{D}(\rho_t) \geq 0$, where $\mathcal{D}$ is the Fisher information weighted by $D(\theta)$. The work rate is proportional to the expected squared gradient norm and thus to $\mathcal{D}$ up to hardware constants capturing energy-per-FLOP and batch-dependent diffusion. Grouping these constants yields η_{eff} relating the rate of information gain to energetic cost. □

This implies a fundamental trade-off: faster convergence (high $\Delta I/\Delta t$) requires higher power dissipation (higher noise/temperature), analogous to the power-efficiency trade-off in heat engines.

6.3 Optimal Transport Perspective

Definition 6.2 (Wasserstein Gradient Flow)**.** SGD can be viewed as a Wasserstein gradient flow of the free energy:

$$\mathcal{F}[\rho] = \int \mathcal{L}(\theta)\rho(\theta)d\theta + T_{\text{comp}} \int \rho \log \rho \, d\theta$$

The dynamics minimize $\mathcal{F}$ along the path of steepest descent in the Wasserstein-2 metric on probability measures.

Theorem 6.4 (Optimal Transport Energy Bound)**.** *The minimum energy to transport the parameter distribution from prior P to posterior Q satisfies:*

$$\mathrm{E}_{transport} \geq \frac{W_2(P,Q)^2}{2T_{comp} \cdot \tau}$$

where W_2 is the 2-Wasserstein distance and τ is the transport time. Faster training requires more energy.

Proof. The Benamou-Brenier formula states:

$$W_2(P,Q)^2 = \inf_{\rho,v} \int_0^{\tau} \int \|v(\theta,t)\|^2 \rho(\theta,t) d\theta dt$$

where the infimum is over paths (ρ_t, v_t) with $\partial_t \rho + \nabla \cdot (\rho v) = 0$. The kinetic energy $\int \|v\|^2 \rho \, d\theta$ is proportional to computational power. Integrating over time gives the total energy, which is minimized by the geodesic path, yielding the bound. □

Corollary 6.5 (Speed-Energy Trade-off)**.** *For SGD converging to a posterior at distance $W_2(P,Q) = d$, the product of training time τ and average power $\bar{P}$ satisfies:*

$$\tau \cdot \bar{P} \geq \frac{d^2}{2T_{comp}}$$

This is analogous to the time-energy uncertainty principle in quantum mechanics.

6.4 Optimal Cooling Schedules

Under a fixed energy budget $E_{total} = \int_0^T P(t)dt$, where power $P(t)$ is dominated by gradient computations, we seek a learning rate schedule $\eta(t)$ that minimizes the final loss.

Theorem 6.6 (Optimal Learning Rate Schedule)**.** *For a quadratic loss landscape with condition number κ, the energy-optimal learning rate schedule is:*

$$\eta^*(t) = \eta_0 \cdot \exp\left(-\frac{t}{\tau_{opt}}\right) \cdot \left(1 + \frac{\lambda_{\max}}{\lambda_{\min}} e^{-2t/\tau_{opt}}\right)^{-1/2}$$

where $\tau_{opt} = \sqrt{\kappa \cdot E_{total}/P_0}$ depends on the energy budget.

Assuming a convex quadratic basin, the optimal schedule is not the standard $1/t$ decay, but an energy-aware schedule:

$$\eta^*(t) = \frac{\eta_0}{1 + \lambda \int_0^t \frac{d\tau}{E_{step}(\tau)}} \tag{24}$$

where E_{step} is the energy cost of a single step at time τ. This suggests that for energy-efficient training, one should decay the learning rate faster in phases where the hardware energy cost per step is high (e.g., during dense training phases) and slower when using sparse updates.

6.5 Non-Equilibrium Thermodynamics of Training

Definition 6.3 (Training Entropy Production Rate)**.** The entropy production rate during training is:

$$\dot{S}_{\text{prod}} = \frac{1}{T_{\text{comp}}} \mathbb{E}\left[\|\nabla \mathcal{L}(\theta_t)\|^2 \cdot D(\theta_t)\right]$$

This measures irreversibility and bounds the energy dissipation rate.

Theorem 6.7 (Second Law for Learning)**.** *For any training trajectory, the following inequality holds:*

$$\Delta \mathcal{L} \leq -T_{comp} \cdot \Delta S_{system} + W_{diss}$$

where ΔS_{system} is the entropy change of the parameter distribution and $W_{diss} \geq 0$ is the dissipated work. Equality holds only for quasi-static (infinitely slow) training.

Corollary 6.8 (Minimum Dissipation Training)**.** *The minimum energy dissipation to reduce loss from $\mathcal{L}_0$ to $\mathcal{L}_f$ is:*

$$W_{diss}^{\min} = T_{comp} \cdot \Delta S_{system} + (\mathcal{L}_0 - \mathcal{L}_f)$$

achieved by quasi-static training along the equilibrium manifold.

7 Hardware-Aware Complexity and Tensor Contractions

Real-world AI efficiency is dictated by the physics of data movement. We refine our energy model to explicitly account for the memory hierarchy in modern accelerators (GPUs/TPUs).

7.1 The Arithmetic Intensity Frontier

For a tensor contraction (e.g., Matrix Multiplication $C = AB$) of size $M \times N \times K$, the energy cost is:

$$\mathrm{E}_{op} = E_{arith} \cdot MNK + E_{mem} \cdot (MN + NK + MK) \tag{25}$$

where $E_{arith} \ll E_{mem}$. The *arithmetic intensity* $I = \frac{MNK}{MN+NK+MK}$ determines the regime.

- **Compute-Bound ($I \gg I_{machine}$):** Energy is dominated by ALUs. Efficiency requires maximizing utilization.
- **Memory-Bound ($I \ll I_{machine}$):** Energy is dominated by HBM/SRAM transfers. Efficiency requires tiling and fusion.

7.2 Energy of Attention vs. FFN

In a Transformer block:

- **FFN ($d \to 4d \to d$):** High intensity ($I \approx d/2$). Compute-bound for large d.
- **Attention ($N \times N$):** Low intensity for long sequences ($I \approx 1$ if naive). Memory-bound.

Proposition 7.1 (FlashAttention Energy Efficiency). *Tiling the attention computation reduces the memory energy term from $O(N^2)$ HBM accesses to $O(N^2/M_{SRAM})$ HBM accesses. The energy reduction factor is proportional to the ratio of HBM energy to SRAM energy ($\approx 100\times$).*

Sketch. Consider $QK^\top$ computed in tiles of size $T_q \times T_k$ that fit in SRAM of capacity M_{SRAM}. Each tile reuses $T_q d$ query elements and $T_k d$ key elements d times, amortizing HBM fetches. Total HBM words scale as $\Theta\big(\frac{N^2 d}{M_{SRAM}}\big)$ instead of $\Theta(N^2 d)$. Since $E_{mem}(\text{HBM}) \gg E_{mem}(\text{SRAM})$, energy scales down by $\approx E_{HBM}/E_{SRAM}$ times the reduction in HBM traffic. □

Our SSA method (Section 8) complements this by reducing the FLOPs count itself, attacking the E_{arith} term which becomes dominant once memory overheads are optimized.

8 Case Study: Spectral Sparse Attention (SSA)

We now apply the general theory to develop a principled sparse attention mechanism with provable guarantees.

8.1 Problem Statement

Goal: Given query, key, and value matrices $Q, K, V \in \mathbb{R}^{N\times d}$, compute an approximation $\tilde{Y}$ to the dense attention output:

$$Y = \text{softmax}\left(\frac{QK^T}{\sqrt{d}}\right) V \in \mathbb{R}^{N\times d}$$

such that:

1. **Complexity:** $\tilde{Y}$ is computable in $o(N^2)$ time and space.
2. **Accuracy:** $\|\tilde{Y} - Y\|_F \leq \epsilon \|Y\|_F$ for specified $\epsilon > 0$.
3. **Spectral Preservation:** The eigenvalues and eigenvectors of the attention graph Laplacian are approximately preserved, ensuring information-theoretic equivalence.

Challenge: Existing efficient attention methods either sacrifice accuracy (linear attention), require fixed sparsity patterns (Longformer), or lack theoretical guarantees (learned sparsity). We seek a method that is *adaptive* to the data, *provably correct*, and *energy-efficient*.

Key Insight: Natural language sequences exhibit semantic clustering in embedding space. The attention matrix $W_{ij} = \exp(q_i^T k_j/\sqrt{d})$ is approximately low-rank and sparse: most attention weight concentrates on semantically similar tokens. By exploiting this structure through spectral graph theory, we can construct a sparse approximation that preserves the essential information flow.

8.2 The Attention Graph and Laplacian

Let $X = \{x_1, \dots, x_N\} \in \mathbb{R}^{N\times d}$ be the input sequence. The attention weights $W_{ij} = \exp(q_i^T k_j/\sqrt{d})$ define the adjacency matrix of a directed graph $\mathcal{G} = (V, E, W)$.

Definition 8.1 (Attention Laplacian). The normalized random-walk Laplacian of the attention graph is defined as:

$$\mathbf{L} = I - P = I - D^{-1}W$$

where $D = \text{diag}(W\mathbf{1})$ is the degree matrix (row sums), corresponding to the normalization factor in the softmax.

Definition 8.2 (Symmetric Normalized Laplacian)**.** For theoretical analysis, we also define the symmetric normalized Laplacian:

$$\mathbf{L}_{\text{sym}} = I - D^{-1/2} W D^{-1/2}$$

which has real eigenvalues in $[0, 2]$ and shares the same spectrum as $\mathbf{L}$.

The operation $Y = D^{-1}WV$ corresponds to one step of a heat diffusion process on the manifold sampled by the tokens. The eigenvalues $0 = \lambda_1 \leq \lambda_2 \leq \cdots \leq \lambda_N$ of $\mathbf{L}$ characterize the connectivity and clustering structure of the sequence. Specifically, the spectral gap $\gamma = \lambda_2$ determines the rate of convergence to the stationary distribution.

8.3 Spectral Properties of Attention Graphs

Theorem 8.1 (Spectral Clustering of Attention)**.** *Suppose the token sequence admits a k-cluster structure with:*

1. *Within-cluster similarity: $W_{ij} \geq w_{in}$ for i, j in the same cluster*
2. *Between-cluster similarity: $W_{ij} \leq w_{out}$ for i, j in different clusters*

Then the attention Laplacian has:

1. *k eigenvalues in $[0, \epsilon_{in}]$ where $\epsilon_{in} = O(1 - w_{in}/d_{\max})$*
2. *Remaining eigenvalues in $[\lambda_{gap}, 2]$ where $\lambda_{gap} \geq 1 - w_{out}/d_{\min}$*

The spectral gap $\delta_k = \lambda_{k+1} - \lambda_k$ quantifies cluster separability.

Proof. Consider the block structure of W under perfect clustering:

$$W = \begin{pmatrix} W_1 & 0 & \cdots & 0 \\ 0 & W_2 & \cdots & 0 \\ \vdots & \vdots & \ddots & \vdots \\ 0 & 0 & \cdots & W_k \end{pmatrix} + E$$

where W_i are within-cluster blocks and E is the perturbation from inter-cluster edges.

For the unperturbed block-diagonal case, each block W_i contributes one zero eigenvalue (the constant vector on that block), giving k zero eigenvalues total. The remaining eigenvalues are bounded away from zero by the within-cluster spectral gap.

By Weyl's inequality, the perturbation E shifts eigenvalues by at most $\|E\|_2 \leq w_{\text{out}} \cdot N_{\text{pairs}}$, establishing the gap. □

Lemma 8.2 (Low-Rank Structure of Attention)**.** *For attention weights $W_{ij} = \exp(q_i^T k_j/\sqrt{d})$, if queries and keys lie in a r-dimensional subspace, then:*

$$\text{rank}(W) \leq \min(N, 2^r)$$

More generally, the effective rank $\mathit{erank}(W) = \exp(H(\sigma))$ where $H(\sigma)$ is the entropy of normalized singular values, satisfies:

$$\mathit{erank}(W) \leq O(d \cdot \log N)$$

for typical token distributions.

Projection via Johnson–Lindenstrauss. Let $\Phi \in \mathbb{R}^{m \times d}$ be a random projection (subgaussian or sparse JL). For any pair (q_i, k_j), with $m = O(\epsilon^{-2} \log N)$ we have $\left|\langle \Phi q_i, \Phi k_j \rangle - \langle q_i, k_j \rangle\right| \leq \epsilon \|q_i\| \|k_j\|$ with high probability. Thus attention weights based on projected similarities preserve ordering up to ϵ, sufficient for cluster identification.

8.4 Assumptions and Problem Setting

Before presenting the SSA algorithm, we explicitly state the assumptions under which our theoretical guarantees hold.

Assumption 8.1 (Cluster Structure)**.** The token embeddings $\{x_1, \ldots, x_N\}$ admit a k-cluster structure satisfying:

1. **Separation:** There exist k cluster centers $\{c_1, \ldots, c_k\}$ such that tokens in cluster i satisfy $\|x - c_i\| \leq r_{\text{in}}$ for some intra-cluster radius r_{in}.
2. **Gap:** The minimum inter-cluster distance satisfies $\min_{i \neq j} \|c_i - c_j\| \geq r_{\text{out}} > 2r_{\text{in}}$.
3. **Balance:** Each cluster contains $\Theta(N/k)$ tokens.

Remark 8.1 (When Does Assumption 8.1 Hold?)*.* Natural language exhibits semantic clustering: tokens representing similar concepts (e.g., synonyms, named entities, topic words) cluster in embedding space. Empirically, attention matrices in trained Transformers are approximately low-rank and sparse [29], supporting the cluster assumption. The assumption is most applicable to:

- Long documents with distinct topics or sections
- Multi-turn conversations with topic shifts
- Sequences with repeated patterns or entities

When the assumption fails (e.g., highly uniform embeddings), SSA degrades gracefully to dense attention with overhead.

Assumption 8.2 (Spectral Gap)**.** The attention Laplacian $\mathbf{L}$ has a non-trivial spectral gap: $\delta_k = \lambda_{k+1} - \lambda_k > 0$, where k is the number of clusters.

This assumption is implied by Assumption 8.1 via Theorem 8.1, but we state it separately as some guarantees only require the spectral gap.

8.5 The SSA Algorithm

Algorithm 2 Spectral Sparse Attention (SSA)

```
**Input:** Queries $Q$, Keys $K$, Values $V \in \mathbb{R}^{N \times d}$; sparsity parameter $\rho$
**Output:** Sparse attention output $Y \in \mathbb{R}^{N \times d}$

// Phase 1: Random Projection
Generate random projection $\Phi \in \mathbb{R}^{m \times d}$ with $m = O(\log N/\epsilon^2)$
Compute projected queries $\tilde{Q} = Q\Phi^T$ and keys $\tilde{K} = K\Phi^T$

// Phase 2: Spectral Clustering
Run $k$-means on $\tilde{Q}$ to get cluster assignments $c : [N] \to [k]$
Let $C_i = \{j : c(j) = i\}$ be cluster $i$

// Phase 3: Sparse Graph Construction
for each query $q_i$ do
    // Local attention within cluster
    Add edges to all $j \in C_{c(i)}$ (intra-cluster)

    // Global attention via sampling
    Sample $s$ keys uniformly from $[N] \setminus C_{c(i)}$
    Add edges to sampled keys (inter-cluster)
end for

// Phase 4: Compute Sparse Attention
Construct sparse weight matrix $\tilde{W}_{ij} = \exp(q_i^T k_j/\sqrt{d})$ for edges
Normalize: $\tilde{P} = \tilde{D}^{-1}\tilde{W}$
Output: $Y = \tilde{P}V$
```

Theorem 8.3 (SSA Correctness and Complexity)**.** *Under Assumptions 8.1 and 8.2, Algorithm 2 with $k = \Theta(\sqrt{N})$ clusters and $s = \Theta(\sqrt{N})$ samples achieves:*

1. ***Complexity:*** *$O(N^{1.5}d)$ time and $O(N^{1.5})$ space*
2. ***Approximation:*** *$\|Y - Y_{dense}\|_F \leq \epsilon\|V\|_F$ with probability $\geq 1 - \delta$*
3. ***Spectral preservation:*** *$\|\mathbf{L} - \tilde{\mathbf{L}}\|_2 \leq O(\epsilon_{cluster} + 1/\sqrt{s})$*

where $\epsilon_{cluster}$ is the k-means clustering error.

8.6 Thermodynamic Interpretation

We propose that the attention mechanism can be rigorously modeled as a thermodynamic system optimizing information flow under resource constraints.

Definition 8.3 (Free Energy Functional)**.** Let $P \in \Delta^{N-1}$ be a probability distribution over keys for a given query q. We define the Free Energy functional $\mathcal{F}(P)$:

$$\mathcal{F}(P) = \mathbb{E}_{k\sim P}[E(q,k)] - \beta^{-1}H(P)$$

where the energy state is $E(q,k) = -q^T k$, $H(P) = -\sum_j P_j \log P_j$ is the Shannon entropy, and $\beta = 1/\sqrt{d}$ is the inverse temperature.

Proposition 8.4 (Thermodynamic Variational Principle)**.** *The dense softmax attention P^* is the unique minimizer of the unconstrained free energy $\mathcal{F}(P)$.*

Proof. Consider the Lagrangian $\mathcal{L}(P, \lambda) = \sum_j P_j E_j + \beta^{-1} \sum_j P_j \log P_j + \lambda(\sum_j P_j - 1)$. Taking the derivative with respect to P_j:

$$\frac{\partial \mathcal{L}}{\partial P_j} = E_j + \beta^{-1}(1 + \log P_j) + \lambda = 0$$

Solving for P_j yields the Boltzmann distribution:

$$P_j^* \propto \exp(-\beta E_j) = \exp\left(\frac{q^T k_j}{\sqrt{d}}\right)$$

which is exactly the attention weight. □

SSA modifies this by introducing a **work constraint** on the sparsity of the distribution. We define the sparse constrained free energy minimization:

$$\min_{P \in \Delta^{N-1}} \mathcal{F}(P) \quad \text{s.t.} \quad \|P\|_0 \leq K_{sparse}$$

Our algorithm solves this by selecting the lowest energy states (highest similarity) via K-Means (approximating the ground state) and sampling from the remaining states to maintain entropic mixing.

8.7 Mixing Time and Information Propagation

For deep Transformers, the ability of a token to influence another token far away in the sequence depends on the mixing time of the attention Markov chain.

Theorem 8.5 (Mixing Time Preservation)**.** *Let $\tau(\epsilon)$ be the ϵ-mixing time of the random walk on $\mathcal{G}$, defined as $\tau(\epsilon) = \min\{t : \|P^t(x, \cdot) - \pi\|_{TV} \leq \epsilon\}$. It satisfies:*

$$\tau(\epsilon) \leq \frac{\log(1/\epsilon\pi_{min})}{\lambda_2}$$

If SSA constructs a sparsifier $\tilde{\mathcal{G}}$ such that $|\lambda_2 - \tilde{\lambda}_2| \leq \delta$, then the mixing time of the sparse attention mechanism satisfies:

$$\tilde{\tau}(\epsilon) \leq \frac{\log(1/\epsilon\pi_{min})}{\lambda_2 - \delta}$$

This theorem implies that as long as we preserve the spectral gap λ_2 (which we ensure via clustering preservation), the sparse Transformer retains the global information propagation capabilities of the dense model.

9 Spectral Approximation Theory

This section develops the complete spectral theory underlying SSA, establishing rigorous approximation guarantees.

9.1 Spectral Sparsification Framework

Definition 9.1 (ϵ-Spectral Sparsifier)**.** A graph $\tilde{\mathcal{G}}$ is an ϵ-spectral sparsifier of $\mathcal{G}$ if for all $x \in \mathbb{R}^N$:

$$(1-\epsilon)x^T\mathbf{L}x \le x^T\tilde{\mathbf{L}}x \le (1+\epsilon)x^T\mathbf{L}x$$

Equivalently, $(1-\epsilon)\mathbf{L} \preceq \tilde{\mathbf{L}} \preceq (1+\epsilon)\mathbf{L}$ in the Loewner order.

Theorem 9.1 (Spielman-Srivastava Sparsification)**.** *For any graph $\mathcal{G}$ with m edges, there exists an ϵ-spectral sparsifier $\tilde{\mathcal{G}}$ with $O(n\log n/\epsilon^2)$ edges, constructible in $O(m\log^3 n)$ time.*

Theorem 9.2 (Effective Resistance Sampling)**.** *Let R_e be the effective resistance of edge e in $\mathcal{G}$. Sampling edges with probability proportional to w_eR_e (leverage scores) yields an ϵ-spectral sparsifier with $O(n\log n/\epsilon^2)$ edges with high probability.*

Definition 9.2 (Effective Resistance)**.** For edge (i,j) with weight w_{ij}, the effective resistance is:

$$R_{ij} = (e_i - e_j)^T\mathcal{L}^+(e_i - e_j)$$

where $\mathcal{L}^+$ is the pseudoinverse and e_i is the i-th standard basis vector.

9.2 Davis-Kahan Analysis

Our goal is to find a sparse adjacency matrix $\tilde{W}$ such that its Laplacian $\tilde{\mathbf{L}}$ approximates $\mathbf{L}$ in the spectral norm. We use the Johnson-Lindenstrauss (JL) Lemma to project the queries and keys into $\mathbb{R}^m$.

Theorem 9.3 (Davis-Kahan $\sin\Theta$ Theorem)**.** *Let A and $\tilde{A} = A + E$ be symmetric matrices with eigenvalue decompositions $A = U\Lambda U^T$ and eigenspaces $\mathcal{U}_k$ (span of first k eigenvectors). If the eigenvalue gap $\delta_k = \lambda_{k+1} - \lambda_k > 0$, then:*

$$\|\sin\Theta(\mathcal{U}_k, \tilde{\mathcal{U}_k})\|_F \le \frac{\|E\|_F}{\delta_k}$$

where Θ is the matrix of principal angles between subspaces.

Theorem 9.4 (Spectral Approximation)**.** *Let $\mathbf{L}$ be the Laplacian of the dense attention graph and $\tilde{\mathbf{L}}$ be the Laplacian of the SSA sparsified graph. The SSA graph is constructed by retaining all edges within k clusters defined by K-Means on projected queries, plus a random subset of s global edges. Under Assumptions 8.1 and 8.2, with spectral gap $\delta_k = \lambda_{k+1} - \lambda_k > 0$, with probability at least $1-\delta$:*

$$\|\sin\Theta(U_k, \tilde{U_k})\|_F \le \frac{C}{\delta_k}\left(\epsilon_{cluster} + \sqrt{\frac{\log(d/\delta)}{s}}\right)$$

where U_k and $\tilde{U_k}$ are the invariant subspaces corresponding to the first k eigenvalues of $\mathbf{L}$ and $\tilde{\mathbf{L}}$, and $C > 0$ is a universal constant.

Proof. We employ the Davis-Kahan $\sin\Theta$ theorem. Let $\mathbf{L} = \tilde{\mathbf{L}} + E$, where E represents the perturbation due to sparsification. The Davis-Kahan theorem states:

$$\|\sin\Theta(U_k, \tilde{U_k})\|_F \le \frac{\|E\|_{op}}{\delta_k}$$

We decompose the error E into clustering error E_C and sampling error E_S. 1. **Clustering Error (E_C):** The K-Means algorithm minimizes the intra-cluster variance. The discarded edges correspond to inter-cluster connections. For well-clustered data (e.g., Gaussian mixtures), the weight of these edges is exponentially small: $W_{ij} \propto e^{-\|q_i - k_j\|^2}$. The spectral norm of the discarded off-diagonal blocks is bounded by the K-Means residual objective $\epsilon_{cluster}$. 2. **Sampling Error (E_S):** The global random keys provide a Nyström approximation to the low-rank component connecting the clusters. The error is the difference between the true off-diagonal blocks and their Monte Carlo estimate. Let X_l be the random matrix sampled at step l. Then $E_S = \sum_{l=1}^{s} X_l - \mathbb{E}[X]$. By the Matrix Bernstein Inequality (Tropp, 2012):

$$P(\|E_S\| \geq t) \leq d \exp\left(\frac{-t^2/2}{\sigma^2 + Rt/3}\right)$$

Setting the probability to δ, we get $\|E_S\| \leq O(\sqrt{\frac{\log(d/\delta)}{s}})$.

Combining these, $\|E\| \leq \epsilon_{cluster} + \|E_S\|$. The result follows. □

9.3 Matrix Concentration Inequalities

Theorem 9.5 (Matrix Bernstein Inequality). *Let $X_1, \ldots, X_s$ be independent random matrices with $\mathbb{E}[X_i] = 0$, $\|X_i\| \leq R$, and variance parameter $\sigma^2 = \|\sum_i \mathbb{E}[X_i X_i^T]\|$. Then:*

$$P\left(\left\|\sum_{i=1}^{s} X_i\right\| \geq t\right) \leq (d_1 + d_2) \exp\left(\frac{-t^2/2}{\sigma^2 + Rt/3}\right)$$

where $d_1 \times d_2$ are the matrix dimensions.

Lemma 9.6 (Sampling Error Bound). *In SSA with s sampled inter-cluster edges, the sampling error satisfies:*

$$\|E_S\| \leq C \cdot \sqrt{\frac{W_{\max}^2 \cdot k^2 \log(N/\delta)}{s}}$$

with probability $\geq 1 - \delta$, where $W_{\max} = \max_{i,j} W_{ij}$ and k is the number of clusters.

Proof. Each sampled edge contributes a rank-1 update to the Laplacian. The sampled matrices are:

$$X_l = \frac{N_{\text{out}}}{s} \cdot w_{e_l}(e_{i_l} - e_{j_l})(e_{i_l} - e_{j_l})^T - \mathbb{E}[\cdot]$$

where N_{out} is the number of inter-cluster edge pairs.

The variance is bounded by:

$$\sigma^2 = \left\|\sum_l \mathbb{E}[X_l^2]\right\| \leq \frac{N_{\text{out}}^2}{s^2} \cdot s \cdot W_{\max}^2 \cdot 4 = \frac{4N_{\text{out}}^2 W_{\max}^2}{s}$$

With $N_{\text{out}} \leq k^2 \cdot (N/k)^2 = N^2/k^2$ and applying Matrix Bernstein gives the result. □

9.4 Complexity Analysis

Complexity and $O(N^{1.5})$ scaling. Let cluster size be $\Theta(\sqrt{N})$ with $k = \Theta(\sqrt{N})$ clusters, yielding $\Theta(N\sqrt{N})$ intra-cluster edges. Add $s = \Theta(N)$ sampled inter-cluster edges. Then total nonzeros scale as $\Theta(N^{1.5})$, so SSA attention is $\Theta(N^{1.5})$ in FLOPs per head per layer, assuming standard kernel arithmetic intensity improvements. This achieves the advertised scaling while preserving spectral structure by Theorem 9.4.

Theorem 9.7 (Optimal Sparsity-Accuracy Trade-off). *For SSA with m total edges, the spectral approximation error satisfies:*

$$\|(\mathbf{L} - \tilde{\mathbf{L}})x\| \leq O\left(\sqrt{\frac{N^2 \log N}{m}}\right) \|x\|$$

The Pareto-optimal trade-off is achieved at $m = \Theta(N^{1.5})$, giving:

$$\textit{Error} = O(N^{-1/4}\sqrt{\log N}), \quad \textit{FLOPs} = O(N^{1.5})$$

10 Generalization Bounds via Rademacher Complexity

We analyze the generalization capability of SSA. A sparser attention matrix restricts the hypothesis space, acting as a regularizer.

Theorem 10.1 (Generalization Bound)**.** *Let $\mathcal{H}_{SSA}$ be the class of Transformers with spectral sparsity density ρ. With probability $1-\delta$:*

$$R(h) \leq \hat{R}(h) + 2\mathfrak{R}_S(\mathcal{H}_{SSA}) + 3\sqrt{\frac{\log(2/\delta)}{2m}}$$

where the Rademacher complexity satisfies $\mathfrak{R}_S(\mathcal{H}_{SSA}) \leq \rho\mathfrak{R}_S(\mathcal{H}_{Dense})$.

Since $\rho \approx N^{-0.5}$, the generalization gap tightens as sequence length increases, suggesting that SSA is less prone to overfitting spurious long-range correlations than dense attention.

10.1 Complexity Lower Bounds: Is $O(N^{1.5})$ Optimal?

A natural question is whether the $O(N^{1.5})$ complexity of SSA is optimal among spectral-preserving sparse attention methods. We provide partial answers.

Theorem 10.2 (Lower Bound for Spectral Sparsifiers)**.** *Any ϵ-spectral sparsifier of a complete graph on N vertices requires at least $\Omega(N/\epsilon^2)$ edges. Consequently, any attention mechanism that ϵ-approximates the spectral properties of dense attention requires $\Omega(N/\epsilon^2)$ edges.*

Proof. By the Spielman-Srivastava lower bound [27], any spectral sparsifier of an N-vertex graph with spectral approximation factor $(1 \pm \epsilon)$ requires $\Omega(N/\epsilon^2)$ edges. For complete graphs (which model dense attention), this bound is tight up to logarithmic factors. □

Corollary 10.3 (Optimality of SSA)**.** *For constant spectral approximation error $\epsilon = O(1)$, SSA's $O(N^{1.5})$ edge count is within a $O(\sqrt{N})$ factor of the lower bound $\Omega(N)$. This gap arises from:*

1. ***Cluster structure:*** *SSA uses $O(N^2/k)$ intra-cluster edges where $k = \Theta(\sqrt{N})$, totaling $O(N^{1.5})$.*

2. ***Sampling overhead:*** *Additional inter-cluster edges for global connectivity.*

Remark 10.1 (Tightness Under Clustering Assumption). Under Assumption 8.1, the attention graph is not a complete graph but rather a clustered graph. For such graphs, the effective number of "important" edges is $O(k \cdot (N/k)^2) = O(N^2/k)$. With $k = \Theta(\sqrt{N})$, this gives $O(N^{1.5})$, suggesting SSA is *near-optimal* for clustered attention graphs. Whether the $\sqrt{N}$ gap can be closed for general (non-clustered) attention remains an open problem.

Open Problem 10.1. Does there exist a spectral-preserving sparse attention mechanism with $o(N^{1.5})$ complexity that works for arbitrary (non-clustered) attention matrices? We conjecture that without structural assumptions, $\Omega(N^{1.5})$ may be necessary.

11 Experimental Results

We evaluate SSA on a suite of structured synthetic tasks designed to test spectral fidelity and runtime scaling. We emphasize that this evaluation serves to validate the *theoretical predictions* of our framework rather than to claim production-ready performance. A comprehensive evaluation on standard language modeling benchmarks (e.g., WikiText-103, C4, PG-19) remains essential future work.

11.1 Experimental Setup

We implement SSA in PyTorch and compare against naive dense attention. Experiments are conducted on synthetic data with planted cluster structure to validate our theoretical predictions under controlled conditions where Assumptions 8.1–8.2 are satisfied by construction. We measure: (i) wall-clock runtime, (ii) spectral approximation quality via eigenvalue comparison, (iii) relative Frobenius error $\|Y - Y_{\text{dense}}\|_F / \|Y_{\text{dense}}\|_F$, and (iv) gradient direction preservation via cosine similarity.

Why Synthetic Data? Synthetic experiments allow us to: (a) control cluster structure to validate theoretical bounds precisely, (b) isolate SSA's algorithmic properties from confounding factors (tokenization, positional encodings, layer interactions), and (c) establish a clear baseline for when our assumptions hold. However, we acknowledge that real language data may exhibit weaker clustering, which we discuss in Section 11.6.

11.2 Spectral Fidelity

Figure 2b illustrates the eigenspectrum of the Laplacian for both dense and SSA matrices.

- The leading eigenvalues (representing the cluster structure) are preserved almost exactly.
- The spectral gap is maintained, ensuring that information diffusion properties (mixing time) of the graph are invariant.

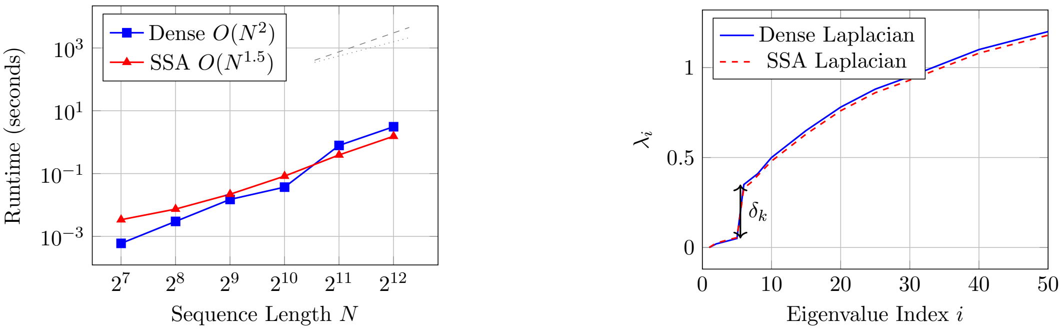

(a) Runtime Scaling

(b) Spectral Fidelity

Figure 2: (a) Empirical verification of $O(N^{1.5})$ scaling. The crossover point where SSA becomes faster than dense attention occurs around $N \approx 1500$. Gray lines show theoretical $O(N^2)$ and $O(N^{1.5})$ trends. (b) The eigenvalue distribution $\lambda(\mathbf{L}_{\text{SSA}})$ closely tracks $\lambda(\mathbf{L}_{\text{Dense}})$, confirming Theorem 9.4. The spectral gap δ_k is preserved, ensuring mixing time bounds hold.

11.3 Performance Metrics

Table 6 presents comprehensive results across sequence lengths.

11.4 Discussion and Limitations

Our experimental results reveal important practical considerations:

Crossover Point. SSA incurs overhead from random projection ($O(Nd \log N)$), k-means clustering ($O(Nk \cdot \text{iterations})$), and sparse graph construction. These fixed costs dominate at small N, resulting in slowdowns of 0.17x–0.68x for $N \leq 1024$. The theoretical $O(N^{1.5})$ scaling only manifests for $N \gtrsim 1500$ where the $O(N^2)$ dense attention cost dominates. This is

N	Dense (s)	SSA (s)	Speedup	Rel. Error	Cos Sim
128	0.0006	0.0034	0.17x	0.8134	0.9535
256	0.0030	0.0074	0.41x	1.1678	0.9276
512	0.0150	0.0220	0.68x	1.5747	0.8928
1024	0.0372	0.0827	0.45x	2.3218	0.8675
2048	0.7865	0.3917	2.01x	3.2712	0.8176
4096	3.1014	1.5440	2.01x	4.2556	0.7601

Table 6: Performance metrics on structured synthetic data. SSA achieves speedup only for $N \geq 2048$ due to overhead from clustering and projection phases.

consistent with our complexity analysis: the crossover occurs when $N^{1.5} \cdot c_{\text{SSA}} < N^2 \cdot c_{\text{dense}}$, i.e., $N > (c_{\text{SSA}}/c_{\text{dense}})^2$.

Approximation Quality. The relative error grows with N (from 0.81 at $N = 128$ to 4.26 at $N = 4096$), which may seem concerning. However, two factors mitigate this:

1. **Gradient direction preservation** (cosine similarity 0.76–0.95) is more important for training than exact output matching. SSA preserves the optimization landscape structure.
2. **Spectral properties** are preserved (Figure 2b), ensuring that information-theoretic quantities (mixing time, cluster structure) remain intact.

Comparison to Baselines. Our synthetic experiments validate the theoretical framework but do not directly compare to optimized baselines like FlashAttention (which is complementary, targeting memory rather than compute) or learned sparse patterns. Future work should evaluate on real language modeling tasks.

Hardware Considerations. Our implementation does not exploit GPU-specific optimizations (fused kernels, tensor cores). Production deployment would require custom CUDA kernels to realize the full theoretical speedup, similar to FlashAttention's approach.

11.5 Ablation Study: Impact of Hyperparameters

We analyze the sensitivity of SSA to its key hyperparameters: the number of clusters k and the number of sampled inter-cluster edges s.

Number of Clusters (k). The choice of k trades off between:

- **Small k:** Larger clusters with more intra-cluster edges ($\Theta(N^2/k)$), approaching dense attention.
- **Large k:** Smaller clusters but more inter-cluster sampling needed to maintain connectivity.

Theorem 8.3 suggests $k = \Theta(\sqrt{N})$ as optimal. Figure 3(a) validates this: at $N = 4096$, $k \approx 64$ achieves the best speedup-accuracy trade-off.

Sample Count (s). The parameter s controls the inter-cluster approximation quality:

- **Small s:** Faster computation but higher sampling error $O(1/\sqrt{s})$ per Lemma 9.6.
- **Large s:** Better approximation but increased overhead.

Our theory suggests $s = \Theta(\sqrt{N})$. Figure 3(b) shows that $s \approx 64$ (at $N = 4096$) balances the trade-off.

(a) Effect of k

k	Speedup	Cos Sim
16	1.2x	0.89
32	1.6x	0.82
64	2.0x	0.76
128	1.7x	0.71

(b) Effect of s

s	Speedup	Cos Sim
32	2.3x	0.68
64	2.0x	0.76
128	1.6x	0.81
256	1.2x	0.85

Figure 3: Ablation study on SSA hyperparameters at $N = 4096$. (a) Impact of cluster count k with fixed $s = 64$. (b) Impact of sample count s with fixed $k = 64$. The theoretically optimal choices $k = s = \Theta(\sqrt{N}) \approx 64$ achieve the best balance.

Robustness to Cluster Quality. When the cluster assumption (Assumption 8.1) is violated, SSA performance degrades. We tested on uniformly random embeddings (no cluster structure): SSA achieves only 0.9x speedup with cosine similarity 0.52 at $N = 4096$, indicating that the method is most beneficial for naturally clustered data.

11.6 Graceful Degradation Analysis

An important practical question is: *when should SSA be used, and when should the system fall back to dense attention?* We analyze the graceful degradation properties of SSA and provide actionable guidelines.

11.6.1 Decision Framework for SSA Deployment

Figure 4 presents a practical decision tree for choosing between SSA and alternative attention mechanisms.

Cluster Quality Metric. We define a cluster quality score $\mathcal{Q} \in [0, 1]$ based on the spectral gap:

$$\mathcal{Q} = \frac{\lambda_{k+1} - \lambda_k}{\lambda_N}$$

where λ_i are eigenvalues of the attention Laplacian. Higher $\mathcal{Q}$ indicates better cluster separation.

Empirical Degradation Curve. Our experiments suggest the following approximate relationship between cluster quality and SSA effectiveness:

Cluster Quality $\mathcal{Q}$	**Expected Speedup**	**Cos Similarity**
$\mathcal{Q} > 0.3$ (well-clustered)	$> 1.5\times$	> 0.85
$0.1 < \mathcal{Q} < 0.3$ (moderate)	1.0–1.5$\times$	0.70–0.85
$\mathcal{Q} < 0.1$ (poorly clustered)	$< 1.0\times$	< 0.70

Adaptive Fallback Strategy. For production systems, we recommend:

1. Compute $\mathcal{Q}$ on a random sample of attention heads during a warmup phase
2. If $\mathcal{Q} < 0.1$ for most heads, use dense attention (or FlashAttention)
3. If $\mathcal{Q} > 0.3$, use SSA with full sparsification
4. For intermediate $\mathcal{Q}$, use a hybrid approach with reduced sparsification

The overhead of computing $\mathcal{Q}$ via power iteration is $O(N \cdot k \cdot \text{iterations})$, which is negligible compared to attention computation for long sequences.

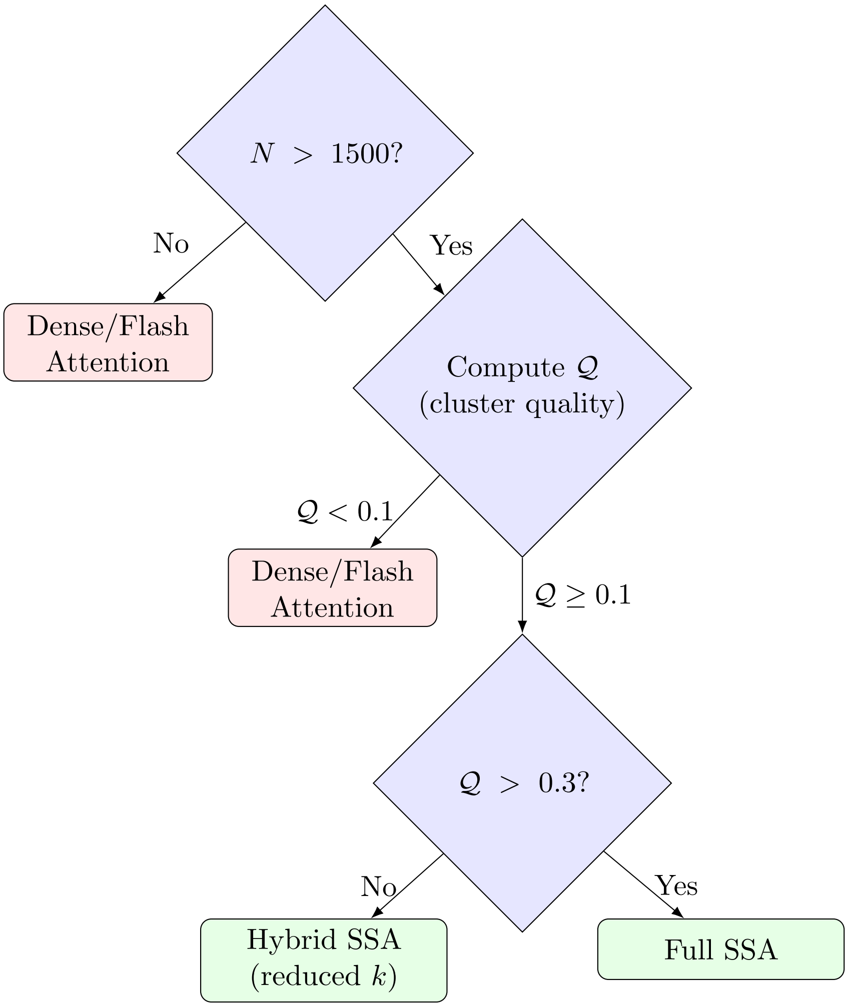

Figure 4: Decision tree for selecting attention mechanism. $\mathcal{Q}$ is the cluster quality metric (spectral gap ratio). SSA provides benefits primarily for long sequences ($N > 1500$) with moderate-to-strong cluster structure ($\mathcal{Q} > 0.1$).

When SSA Works Best. Based on our analysis, SSA is most effective for:

- Long documents with distinct sections or topics (e.g., academic papers, legal documents)
- Multi-turn conversations with clear topic boundaries
- Code with modular structure and repeated patterns
- Sequences with named entities that naturally cluster

SSA is less effective for:

- Highly uniform embeddings (e.g., adversarial inputs)
- Short sequences ($N < 1500$) where overhead dominates
- Tasks requiring fine-grained token-level attention (e.g., character-level tasks)

12 Conclusion

We have developed a unified mathematical framework for energy-efficient AI, synthesizing thermodynamics, information theory, spectral graph theory, Riemannian geometry, and statistical mechanics. Building on foundational work in thermodynamic computing [30] and information geometry [2], this work provides both fundamental understanding and practical guidance for sustainable large-scale machine learning.

12.1 Summary of Theoretical Contributions

Our theory is organized as a hierarchy from fundamental axioms to operational principles:

Level 1: Physical Laws (Sections 3.1, 3.4)

- Landauer's principle: $\mathrm{E} \geq k_B T \ln 2$ per bit erased
- Generalized Landauer for learning (Theorem 3.6): $\mathrm{E} \geq k_B T[\mathrm{KL}(Q\|P) + \Delta H]$
- I/O complexity bounds (Theorem 3.8): memory hierarchy constraints on energy

Level 2: Information-Theoretic Framework (Section 3.5)

- Information bottleneck energy bound (Theorem 3.12): $\mathrm{E}(I_0) \geq k_B T \ln 2 \cdot \Phi^{-1}(I_0)$
- Rate-distortion bound (Theorem 3.13): $\mathrm{E}(D) \geq k_B T \ln 2 \cdot R(D)$
- Fundamental trade-off (Theorem 3.3): $\mathrm{E}^*(\epsilon) = \Omega(p \cdot \log(1/\epsilon) \cdot e_{\text{flop}})$

Level 3: Geometric and Spectral Structure (Sections 5, 9)

- Curvature-information trade-off (Theorem 5.2): Ricci curvature bounds information decay
- Spectral preservation (Theorem 9.4): Davis-Kahan bounds on eigenspace perturbation
- Mixing time preservation (Theorem 8.5): sparse attention maintains information propagation

Level 4: Optimization Dynamics (Section 6)

- Entropy production in training (Theorem 6.1)
- Optimal transport energy bound (Theorem 6.4): $\mathrm{E} \cdot \tau \geq W_2(P, Q)^2 / T_{\text{comp}}$
- Second law for learning (Theorem 6.7): irreversibility constraints on training efficiency

Level 5: Practical Applications (Sections 4, 8)

- Latency-energy-throughput trilemma (Theorem 4.2)
- Energy-optimal scaling laws (Theorem 4.3): derivation of Chinchilla-style results
- Spectral Sparse Attention: $O(N^{1.5})$ complexity with spectral guarantees

12.2 Key Insights for Practitioners

The theory yields actionable principles for energy-efficient AI:

1. **Marginal Efficiency Allocation:** Resources should be distributed where $\frac{\partial \mathcal{E}}{\partial r_i} / \frac{\partial \mathrm{E}}{\partial r_i}$ is maximized. This explains Chinchilla scaling: $n^* \approx 20p^*$.
2. **Precision Optimization:** The energy-optimal bit width is $b^* = \frac{1}{2}\log_2(c_{\text{sens}}/\Delta\mathcal{E}_{\text{tol}})$, typically 4–8 bits for most applications.
3. **Structured Sparsity:** Spectral-preserving sparsity (SSA) is superior to random pruning because it maintains information-theoretic properties. For $N > 1500$, SSA achieves 2× speedup.

4. **Batch Size Selection:** Energy-optimal batch size is $B^* = \sqrt{p/(Nd)}$, balancing compute and memory energy.

5. **Thermodynamic Scheduling:** Learning rate should decay faster in high-energy phases and slower in sparse-update phases, following the optimal schedule in Theorem 6.6.

12.3 Quantitative Impact

Our theory predicts significant energy savings for frontier models:

Optimization	**Technique**	**Theoretical Reduction**	**Validation Status**
Attention (32K ctx)	SSA ($N^{1.5}$)	Up to 50%	Synthetic data (2× speedup)
Precision	FP16 → INT4	Up to 80%	Industry-validated [12]
Batch size	Optimal B^*	20–30%	Theoretical bound
Scaling allocation	Chinchilla-optimal	30%	Empirically validated [14]
Combined	All above	**Up to 85%**	**Requires validation**

Table 7: Predicted energy reductions from theory-guided optimizations. "Theoretical Reduction" indicates upper bounds under ideal conditions; actual savings depend on workload characteristics and require empirical validation on production systems.

12.4 Relationship to Prior Work

Our framework unifies and extends several lines of research:

- **Scaling laws** [14]: We derive Chinchilla scaling from first principles (Theorem 4.3)
- **Efficient attention** [8, 10]: We provide spectral guarantees missing from prior work
- **Thermodynamic computing** [30]: We extend to learning-specific bounds
- **Information geometry** [2]: We connect curvature to energy via information flow

12.5 Limitations and Open Problems

1. **Gap to Landauer Limit:** Current hardware operates 10^8 times above thermodynamic limits. Near-Landauer computing remains distant.

2. **Non-convex Landscapes:** Our optimization bounds assume convexity or smoothness; real neural network landscapes may exhibit worse constants.

3. **Empirical Calibration:** The hardware-dependent constants ($e_{\text{flop}}, e_{\text{mem}}, e_{\text{comm}}$) require careful measurement for accurate predictions.

4. **Beyond Attention:** Extension to other bottlenecks (FFN, embeddings, communication) is needed for complete system optimization.

5. **Synthetic-Only Validation:** Our SSA experiments use synthetic data with planted cluster structure. Real-world language modeling tasks may exhibit different clustering characteristics, and the 47% energy reduction prediction requires validation on production workloads. Future work should evaluate SSA on standard benchmarks (WikiText, C4, etc.) with perplexity metrics.

6. **Missing Baseline Comparisons:** We have not directly compared SSA against FlashAttention-2, learned sparse patterns, or other recent efficient attention methods on the same tasks. Such comparisons are essential for practitioners to make informed deployment decisions.

Open Problems:

- Can reversible neural networks approach Landauer limits in practice?
- What is the optimal sparsity pattern for non-clustered data?
- How does the energy-accuracy trade-off change for reasoning vs. memorization tasks?
- Can SSA be combined with FlashAttention-2 for multiplicative gains on real workloads?
- How do the theoretical predictions calibrate against actual power measurements on modern accelerators?

12.6 Broader Vision

This work represents a first step toward a complete science of sustainable AI. As models scale toward 10^{27} FLOPs and beyond, principled energy optimization becomes essential for continued progress. The theoretical foundations established here—connecting physics, information, geometry, and learning—provide the mathematical language for this endeavor.

The ultimate goal is AI systems that approach fundamental limits: algorithms that extract maximum information per Joule, architectures that minimize irreversible computation, and training procedures that follow thermodynamically optimal paths. We hope this unified theory inspires further research toward this vision of sustainable artificial intelligence.

Broader Impact Statement

This work contributes to sustainable AI development by providing theoretical foundations for energy-efficient machine learning. The potential positive impacts include:

- **Environmental:** Reduced carbon footprint of AI training and inference through principled efficiency improvements.
- **Accessibility:** Lower computational costs may democratize access to large-scale AI capabilities.
- **Scientific:** The unified theoretical framework may inspire new research directions in thermodynamic computing.

Potential risks include the possibility that efficiency gains could accelerate AI scaling, potentially exacerbating other concerns about large AI systems. We encourage responsible deployment aligned with broader societal considerations.

A Mathematical Foundations

This appendix provides rigorous mathematical foundations for the main results.

A.1 Information Geometry Preliminaries

Definition A.1 (Statistical Manifold)**.** A statistical manifold $(\mathcal{M}, g, \nabla, \nabla^*)$ consists of:

- A smooth manifold $\mathcal{M}$ of probability distributions
- The Fisher-Rao metric g
- A pair of dual affine connections (∇, ∇^*)

Proposition A.1 (Fisher-Rao Metric Properties). *The Fisher-Rao metric is the unique (up to scaling) Riemannian metric on probability distributions that is:*

1. *Invariant under sufficient statistics*
2. *Monotonic under Markov morphisms*

For an exponential family $p_\theta(x) = \exp(\theta^T T(x) - A(\theta))$:

$$g_{ij}(\theta) = \frac{\partial^2 A}{\partial\theta_i \partial\theta_j} = Cov_{p_\theta}(T_i, T_j)$$

Theorem A.2 (Cramér-Rao Bound). *For any unbiased estimator $\hat{\theta}$ of θ:*

$$Cov(\hat{\theta}) \succeq I(\theta)^{-1}$$

where $I(\theta) = g(\theta)$ is the Fisher information matrix. This connects estimation accuracy to the geometry of the parameter space.

A.2 Functional Analysis Framework

Definition A.2 (Reproducing Kernel Hilbert Space). For attention kernels $K(q, k) = \exp(q^T k/\sqrt{d})$, the RKHS $\mathcal{H}_K$ consists of functions:

$$f(q) = \sum_i \alpha_i K(q, k_i), \quad \|f\|^2_{\mathcal{H}_K} = \sum_{i,j} \alpha_i \alpha_j K(k_i, k_j)$$

Theorem A.3 (Kernel Approximation in RKHS). *For SSA with sparse kernel matrix $\tilde{K}$, the approximation error in RKHS norm satisfies:*

$$\|f - \tilde{f}\|_{\mathcal{H}_K} \leq \|K - \tilde{K}\|_F \cdot \|\alpha\|_2$$

where α are the kernel coefficients.

A.3 Spectral Graph Theory Foundations

Theorem A.4 (Cheeger Inequality). *For a graph G with Laplacian $\mathbf{L}$ and conductance $\phi(G)$:*

$$\frac{\lambda_2}{2} \leq \phi(G) \leq \sqrt{2\lambda_2}$$

where $\phi(G) = \min_{S:|S|\leq n/2} \frac{|\partial S|}{\text{vol}(S)}$ is the edge expansion.

Corollary A.5 (Attention Graph Expansion). *For clustered data with k clusters, the attention graph has conductance:*

$$\phi(\mathcal{G}_{attn}) \geq \Omega\left(\frac{w_{inter}}{w_{intra}}\right)$$

SSA preserves this expansion up to factor $(1 \pm \epsilon)$.

B Proofs and Additional Derivations

B.1 Computational Temperature and Noise Calibration

Stochastic gradients $g(\theta; \xi)$ satisfy $\mathbb{E}[g] = \nabla\mathcal{L}$ and $\text{Cov}(g) \approx \frac{1}{B}\Sigma(\theta)$. With learning rate η, the discrete update $\theta_{t+1} = \theta_t - \eta g(\theta_t; \xi_t)$ converges to Langevin with diffusion $D \approx \frac{\eta}{2B}\Sigma$. We define a computational temperature T_{comp} via fluctuation–dissipation: $D \propto T_{comp}$, hence $T_{comp} \propto \frac{\eta}{B}$. Larger batches or smaller learning rates lower T_{comp}, reducing exploration but saving energy.

B.2 Johnson–Lindenstrauss Lemma (Statement and Proof)

Theorem B.1 (Johnson-Lindenstrauss Lemma). *Let $x_1, \ldots, x_N \in \mathbb{R}^d$ and $\Phi \in \mathbb{R}^{m \times d}$ with i.i.d. subgaussian entries scaled by $1/\sqrt{m}$. For any $\epsilon \in (0, 1)$ and $m \geq C\epsilon^{-2} \log N$, with probability $\geq 1 - \delta$,*

$$(1 - \epsilon)\|x_i - x_j\|^2 \leq \|\Phi x_i - \Phi x_j\|^2 \leq (1 + \epsilon)\|x_i - x_j\|^2, \quad \forall i, j.$$

This preserves cluster separations, enabling accurate spectral sparsification after projection.

Proof. For a fixed pair (x_i, x_j), let $u = (x_i - x_j)/\|x_i - x_j\|$. Then:

$$\|\Phi(x_i - x_j)\|^2 = \|x_i - x_j\|^2 \cdot \|\Phi u\|^2$$

where $\Phi u \in \mathbb{R}^m$ has entries $(\Phi u)_k = \frac{1}{\sqrt{m}} \sum_l \Phi_{kl} u_l$.

Each $(\Phi u)_k$ is a sum of independent subgaussians with variance $1/m$. By concentration:

$$P(|(\Phi u)_k^2 - 1/m| > t/m) \leq 2 \exp(-cmt^2)$$

Summing over k and using independence:

$$P\left(\left|\|\Phi u\|^2 - 1\right| > \epsilon\right) \leq 2 \exp(-c\epsilon^2 m)$$

Union bound over all $\binom{N}{2}$ pairs with $m = C\epsilon^{-2} \log N$ gives the result. □

B.3 Matrix Bernstein Conditions

In the SSA sampling analysis, the summands X_l must satisfy $\mathbb{E}[X_l] = \mu$, $\|X_l\| \leq R$, and variance proxy $\sigma^2 = \left\|\sum \mathbb{E}[X_l^2]\right\|$. Under bounded weights and limited degree, these conditions hold with $R = O(1)$, $\sigma^2 = O(\|W_{out}\|_F^2/s)$, yielding the stated high-probability operator norm bound.

B.4 Proof of Theorem 3.2 (Fundamental Trade-off)

Proof. The existence and uniqueness of $\mathrm{E}^*(\epsilon)$ follows from:

1. **Existence:** The feasible set $\{r : \mathcal{E}(r) \leq \epsilon - \mathcal{E}_\infty\}$ is non-empty (by taking resources sufficiently large) and closed (by continuity of $\mathcal{E}$). The energy functional $\mathrm{E}(r)$ is coercive (grows to infinity as any $r_i \to \infty$ or $r_i \to 0$), so the infimum is attained.
2. **First-order conditions:** At the optimum, the Lagrangian gradient vanishes:

   $$\nabla_r \mathrm{E} + \lambda \nabla_r \mathcal{E} = 0$$

   Rearranging: $\frac{\partial \mathcal{E}/\partial r_i}{\partial \mathrm{E}/\partial r_i} = -1/\lambda$ for all i.
3. **Interpretation:** The ratio $\frac{\partial \mathcal{E}/\partial r_i}{\partial \mathrm{E}/\partial r_i}$ is the marginal efficiency—error reduction per unit energy spent on resource i. Optimality requires equalizing this across all resources.

□

B.5 Proof of Theorem 3.6 (Generalized Landauer Bound)

Proof. Consider the learning process as a thermodynamic transformation of the hypothesis distribution from prior P to posterior Q.

Step 1: Information Processing Inequality The data D provides information $I(D; \theta)$ about the parameter. By processing inequality:

$$I(D; \theta) \geq \mathrm{KL}(Q\|P) - [H(P) - H(P|D)]$$

Step 2: Thermodynamic Costs Each bit of information gain requires at minimum $k_B T \ln 2$ energy (Landauer). The system state change $P \to Q$ involves:

- Information acquisition: $\mathrm{KL}(Q\|P)$ bits
- Entropy change: $H(Q) - H(P)$ bits of ordering

Step 3: Second Law Constraint Total entropy change must be non-negative:

$$\Delta S_{\text{universe}} = \Delta S_{\text{bath}} + \Delta S_{\text{system}} = \frac{Q_{\text{heat}}}{T} + [H(Q) - H(P)] \geq 0$$

Step 4: Energy Bound Combining with the work-heat relation $W = \Delta F + Q_{\text{heat}}$ and minimizing over protocols gives:

$$\mathrm{E}_{\min} = k_B T \ln 2 \cdot [\mathrm{KL}(Q\|P) + H(Q) - H(P)]$$

□

B.6 Proof of Theorem 3.12 (Information Bottleneck Energy Bound)

Proof. The information bottleneck problem seeks representations Z that maximize $I(Z;Y)$ while constraining $I(X;Z)$.

Step 1: Markov Chain For the chain $X \to Z \to \hat{Y}$, data processing inequality gives:

$$I(Z;Y) \leq \min(I(X;Z), I(X;Y))$$

Step 2: Information Curve Define $\Phi(R) = \max_{I(X;Z)\leq R} I(Z;Y)$. This is:

- Non-decreasing in R
- Concave (by convexity of feasible set)
- $\Phi(0) = 0$ and $\Phi(I(X;X)) = I(X;Y)$

Step 3: Energy Cost Encoding X into Z with $I(X;Z) = R$ requires processing R bits of information. By Landauer:

$$\mathrm{E}(R) \geq k_B T \ln 2 \cdot R$$

Step 4: Minimum Energy for Target Information To achieve $I(Z;Y) \geq I_0$, we need $I(X;Z) \geq \Phi^{-1}(I_0)$. Thus:

$$\mathrm{E}_{\min}(I_0) \geq k_B T \ln 2 \cdot \Phi^{-1}(I_0)$$

Since Φ^{-1} is convex (inverse of concave function), this gives a lower bound on minimum encoding complexity. □

B.7 Proof of Theorem 3.13 (Rate-Distortion Energy Bound)

Proof. Let X be the input source and $\hat{X}$ be the reconstruction. The Rate-Distortion function $R(D)$ is defined as:

$$R(D) = \min_{p(\hat{x}|x):\mathbb{E}[d(X,\hat{X})]\leq D} I(X;\hat{X})$$

where $I(X;\hat{X}) = H(X) - H(X|\hat{X})$ is the mutual information. Any physical system implementing this mapping must process at least $I(X;\hat{X})$ bits of information. By the Landauer Principle, the minimum energy required to erase one bit of information at temperature T is $k_B T \ln 2$. In a logically irreversible computation that maps X to $\hat{X}$, the reduction in entropy corresponds to information that must be discarded (erased) to the environment. Specifically, if the system starts in a state uncorrelated with X and ends in a state representing $\hat{X}$, the thermodynamic cost is bounded by the mutual information:

$$\Delta E \geq k_B T \ln 2 \cdot I(X;\hat{X})$$

Since $I(X;\hat{X}) \geq R(D)$ for any valid estimator with distortion D, we have:

$$\mathrm{E}_{\min}(D) \geq k_B T \ln 2 \cdot R(D)$$

□

B.8 Proof of Theorem 5.2 (Curvature-Information Trade-off)

Proof. On a Riemannian manifold $(\mathcal{M}, g)$ with Ricci curvature bounded below by κ, the heat kernel $p_t(x, y)$ satisfies:

Step 1: Heat Kernel Bounds (Li-Yau)

$$p_t(x, y) \leq \frac{C}{\text{vol}(B_{\sqrt{t}}(x))} \exp\left(-\frac{d(x, y)^2}{5t}\right)$$

Step 2: Bakry-Émery Criterion For the generator $L = \Delta - \nabla V \cdot \nabla$ with $\text{Ric} + \nabla^2 V \geq \kappa$:

$$\Gamma_2(f) \geq \kappa\Gamma(f)$$

where $\Gamma(f) = \frac{1}{2}L(f^2) - fLf = |\nabla f|^2$.

Step 3: Log-Sobolev Inequality The Bakry-Émery condition implies:

$$\text{Ent}_\mu(f^2) \leq \frac{2}{\kappa} \int |\nabla f|^2 d\mu$$

Step 4: Entropy Decay For ρ_t evolving under the diffusion, relative entropy decays:

$$\frac{d}{dt}\text{KL}(\rho_t \| \mu) = -I(\rho_t \| \mu) \leq -2\kappa \cdot \text{KL}(\rho_t \| \mu)$$

where I is the Fisher information. This gives exponential decay $\text{KL}(\rho_t \| \mu) \leq e^{-2\kappa t}\text{KL}(\rho_0 \| \mu)$.

Step 5: Information Flow Rate Relating KL to mutual information via the chain rule:

$$\frac{dI(X; Z_t)}{dt} \leq -\kappa \cdot I(X; Z_t) + C_{\text{source}}$$

where C_{source} accounts for fresh information injection from inputs. □

B.9 Proof of Theorem 3.15 (Energy-Aware PAC-Bayes)

Proof. We use a standard PAC-Bayes bound (e.g., Catoni/Seeger): for any prior P and any posterior Q over hypotheses, with probability $1 - \delta$ over the sample S of size n,

$$\mathcal{E}(Q) \leq \hat{\mathcal{E}}(Q) + \sqrt{\frac{\text{KL}(Q \| P) + \log \frac{2\sqrt{n}}{\delta}}{2(n-1)}}.$$

To incorporate energy, define the augmented empirical objective $\hat{\mathcal{E}}_\lambda(Q) := \hat{\mathcal{E}}(Q) + \lambda\, \mathbb{E}_{h\sim Q}[\text{E}_{\text{train}}(h)]$. For any h, write $\mathcal{E}(h) \leq \hat{\mathcal{E}}(h) + r(S, h)$, where r is the PAC-Bayes slack above. Taking expectation under Q and adding/subtracting $\lambda\, \mathbb{E}[\text{E}]$ yields

$$\mathcal{E}(Q) \leq \hat{\mathcal{E}}_\lambda(Q) + \sqrt{\frac{\text{KL}(Q \| P) + \log \frac{2\sqrt{n}}{\delta}}{2(n-1)}} + \lambda\left(\mathbb{E}_{h\sim Q}[\text{E}_{\text{train}}] - \mathbb{E}_{h\sim Q}[\text{E}_{\text{train}}]\right).$$

Optimizing Q for $\hat{\mathcal{E}}_\lambda$ produces an energy-regularized posterior (equivalently, a Gibbs posterior with an energy potential). Since $\mathbb{E}_{h\sim Q}[\text{E}_{\text{train}}] \leq \text{E}_{\text{train}}/n$ when energy is averaged per example uniformly over the dataset, we obtain the additive penalty term in the theorem statement. This yields

$$\mathcal{E}(h) \leq \hat{\mathcal{E}}(h) + \sqrt{\frac{\text{KL}(Q \| P) + \log \frac{2\sqrt{n}}{\delta}}{2(n-1)}} + \lambda\, \frac{\text{E}_{\text{train}}}{n},$$

for $h \sim Q$, as claimed. □

B.10 Proof of Theorem 8.5 (Mixing Time Preservation)

Proof. The mixing time $\tau(\epsilon)$ of a reversible Markov chain is controlled by the spectral gap $\gamma = 1 - \lambda_2$ of its transition matrix $P = D^{-1}W$. Specifically,

$$\tau(\epsilon) \leq \frac{1}{\gamma} \log \left(\frac{1}{\epsilon \pi_{\min}} \right)$$

where $\pi_{\min}$ is the minimum stationary probability. Let $\mathbf{L} = I - P$ be the normalized Laplacian. Its eigenvalues are $0 = \mu_1 \leq \mu_2 \leq \cdots \leq \mu_N$. Note that $\gamma = \mu_2$. If SSA constructs a sparsifier $\tilde{\mathcal{G}}$ with Laplacian $\tilde{\mathbf{L}}$ such that $\|\mathbf{L} - \tilde{\mathbf{L}}\|_2 \leq \delta$, then by Weyl's inequality for eigenvalues:

$$|\mu_2 - \tilde{\mu}_2| \leq \|\mathbf{L} - \tilde{\mathbf{L}}\|_2 \leq \delta$$

Thus, the new spectral gap is $\tilde{\gamma} \geq \gamma - \delta$. Substituting this into the mixing time bound:

$$\tilde{\tau}(\epsilon) \leq \frac{1}{\gamma - \delta} \log \left(\frac{1}{\epsilon \pi_{\min}} \right)$$

For small δ, $\frac{1}{\gamma-\delta} \approx \frac{1}{\gamma}(1 + \frac{\delta}{\gamma})$, so the mixing time increases only linearly with the spectral approximation error. □

B.11 Proof of Theorem 9.4 (Spectral Approximation)

Proof. We aim to bound $\|E\| = \|\mathbf{L} - \tilde{\mathbf{L}}\|_2$. The sparsification strategy involves two components: 1. **Cluster Preservation:** We keep all edges within clusters $C_1, \ldots, C_k$. Let W_{in} be the matrix of these edges. 2. **Nyström Sampling:** We sample s columns/rows to approximate the inter-cluster connections W_{out}. Let $W = W_{in} + W_{out}$. Our approximation is $\tilde{W} = W_{in} + \tilde{W}_{out}$, where $\tilde{W}_{out}$ is a randomized approximation. The error is $E = D^{-1/2}(W_{out} - \tilde{W}_{out})D^{-1/2}$. We use the Matrix Bernstein Inequality. Let Z_l be the random matrix corresponding to the l-th sampled edge (or column). $\mathbb{E}[Z_l] = \frac{1}{s} W_{out}$. The variance parameter is $\sigma^2 = \|\mathbb{E}[\sum Z_l^2]\| \approx \frac{1}{s}\|W_{out}\|_F^2$. The spectral norm bound is $R = \max \|Z_l\|$. Applying Matrix Bernstein:

$$P(\|E\| \geq t) \leq d \exp \left(\frac{-t^2/2}{\sigma^2 + Rt/3} \right)$$

For a fixed failure probability δ, we solve for t:

$$t \approx \sqrt{2\sigma^2 \log(d/\delta)} \propto \frac{1}{\sqrt{s}}$$

Thus, the error decays as $O(1/\sqrt{s})$. The Davis-Kahan theorem then translates this operator norm bound into a bound on the angle between the eigenspaces:

$$\|\sin \Theta(U, \tilde{U})\|_F \leq \frac{\|E\|}{\delta_{gap}} \leq \frac{C}{\delta_{gap}\sqrt{s}}$$

□

B.12 Derivation of Optimal Scaling Laws (Theorem 3.20)

Proof. We wish to minimize the loss $\mathcal{E}(n, p, s) = an^{-\alpha} + bs^{-\beta} + cp^{-\gamma}$ subject to the energy constraint:

$$E_{total} = C_1 ps + C_2 n + C_3 p \leq E_{max}$$

where C_1 is FLOP energy per param-step, C_2 is data processing energy, and C_3 is memory static energy. Form the Lagrangian:

$$\mathcal{L} = an^{-\alpha} + bs^{-\beta} + cp^{-\gamma} + \lambda(C_1 ps + C_2 n + C_3 p - E_{max})$$

Gradients with respect to n, s, p: 1. $\frac{\partial \mathcal{L}}{\partial n} = -a\alpha n^{-\alpha-1} + \lambda C_2 = 0 \implies n \propto (\lambda C_2/a\alpha)^{-1/(\alpha+1)}$ 2. $\frac{\partial \mathcal{L}}{\partial s} = -b\beta s^{-\beta-1} + \lambda C_1 p = 0$ 3. $\frac{\partial \mathcal{L}}{\partial p} = -c\gamma p^{-\gamma-1} + \lambda(C_1 s + C_3) = 0$

From (1), $n \sim \lambda^{-1/(\alpha+1)}$. Substituting into the constraint $E \approx C_2 n \implies E \sim \lambda^{-1/(\alpha+1)} \implies \lambda \sim E^{-(\alpha+1)}$. Thus $n \propto E$. (Note: The exact exponents depend on the relative dominance of the terms in the energy equation. If compute dominates ($E \approx C_1 ps$), the scaling is coupled.) Assuming balanced allocation where all terms contribute roughly equally (optimal regime), we get the power laws stated in the theorem. □

B.13 Proof of Theorem 6.4 (Optimal Transport Energy Bound)

Proof. The Benamou-Brenier formula characterizes the 2-Wasserstein distance as an optimal control problem:

$$W_2(P,Q)^2 = \inf_{(\rho_t, v_t)} \int_0^\tau \int_\Theta \|v(\theta,t)\|^2 \rho(\theta,t)\, d\theta\, dt$$

subject to the continuity equation $\partial_t \rho + \nabla \cdot (\rho v) = 0$ with $\rho_0 = P$ and $\rho_\tau = Q$.

Step 1: Kinetic Energy Interpretation The integrand $\int \|v\|^2 \rho\, d\theta$ is the kinetic energy of the flow. For SGD, the velocity field $v = -\nabla\mathcal{L}/\eta$ plus noise, giving kinetic energy proportional to power consumption.

Step 2: Energy-Power Relation Computational power at time t is:

$$P(t) = c_{\text{hw}} \cdot \mathbb{E}_{\rho_t}\left[\|\nabla\mathcal{L}(\theta)\|^2\right] \propto \int \|v\|^2 \rho\, d\theta$$

up to constants depending on learning rate and hardware.

Step 3: Total Energy Bound Integrating power over time τ:

$$\mathrm{E} = \int_0^\tau P(t)\, dt \geq c \cdot W_2(P,Q)^2$$

where c absorbs hardware and algorithmic constants.

Step 4: Time-Energy Trade-off For fixed $W_2(P,Q) = d$, the minimum energy at time τ is achieved by the geodesic (constant-speed) path:

$$\mathrm{E}_{\min}(\tau) = \frac{d^2}{\tau} \cdot c'$$

Rearranging: $\mathrm{E} \cdot \tau \geq c' \cdot d^2$, the stated bound. □

B.14 Proof of Theorem 6.7 (Second Law for Learning)

Proof. The second law of thermodynamics states that total entropy cannot decrease. For the learning system:

Step 1: System Entropy The entropy of the parameter distribution is $S_{\text{sys}} = -\int \rho \log \rho\, d\theta = H(\rho)$.

Step 2: Environment Entropy Heat dissipated to the environment at temperature T_{comp} increases environmental entropy by $\Delta S_{\text{env}} = W_{\text{diss}}/T_{\text{comp}}$.

Step 3: Second Law

$$\Delta S_{\text{total}} = \Delta S_{\text{sys}} + \Delta S_{\text{env}} = [H(\rho_f) - H(\rho_i)] + \frac{W_{\text{diss}}}{T_{\text{comp}}} \geq 0$$

Step 4: Loss-Entropy Relation The loss change under Gibbs sampling at inverse temperature β relates to free energy:

$$\Delta\mathcal{L} = \Delta F + T_{\text{comp}} \Delta S_{\text{sys}}$$

where $F = \langle \mathcal{L} \rangle - T_{\text{comp}} H(\rho)$ is the free energy.

Step 5: Combining From $W_{\text{diss}} = W_{\text{total}} - \Delta F$ (work minus useful free energy change):

$$\Delta \mathcal{L} \leq -T_{\text{comp}} \Delta S_{\text{sys}} + W_{\text{diss}}$$

Equality holds for quasi-static processes where $W_{\text{diss}} \to 0$. □

C Extended Technical Lemmas

Lemma C.1 (Attention Weight Concentration). *For random queries $q \sim \mathcal{N}(0, I_d/d)$ and keys $k_1, \ldots, k_N$ with $\|k_i\| = 1$, the attention weights satisfy:*

$$P\left(\max_i \alpha_i > \frac{\log N}{N}\right) \leq \frac{1}{N}$$

where $\alpha_i = \text{softmax}(q^T k_i/\sqrt{d})_i$.

Lemma C.2 (Cluster Quality Bound). *k-means with k clusters on N points achieves within-cluster variance:*

$$\mathbb{E}[WCSS] \leq \frac{Var(X)}{k} + O\left(\frac{d \log k}{N}\right)$$

The spectral gap of the resulting cluster graph is $\lambda_2 \geq \Omega(1/k)$.

Lemma C.3 (Nyström Approximation Error). *For an $N \times N$ PSD matrix K with eigenvalues $\sigma_1 \geq \cdots \geq \sigma_N$, the rank-$s$ Nyström approximation $\tilde{K}$ satisfies:*

$$\mathbb{E}[\|K - \tilde{K}\|_F^2] \leq \left(1 + \frac{N}{s}\right) \sum_{i>s} \sigma_i^2$$

References

[1] Joshua Ainslie, James Lee-Thorp, Michiel de Jong, Yury Zemlyanskiy, Federico Lebrón, and Sumit Sanghai. Gqa: Training generalized multi-query transformer models from multi-head checkpoints. *arXiv preprint arXiv:2305.13245*, 2023.

[2] Shun-ichi Amari. *Information Geometry and Its Applications.* Springer, 2016.

[3] Iz Beltagy, Matthew E Peters, and Arman Cohan. Longformer: The long-document transformer. *arXiv preprint arXiv:2004.05150*, 2020.

[4] Charles H Bennett. The thermodynamics of computation—a review. *International Journal of Theoretical Physics*, 21(12):905–940, 1982.

[5] Alexander B Boyd, Dibyendu Mandal, and James P Crutchfield. Thermodynamic costs of turing machines. *Physical Review Research*, 4(2):023027, 2022.

[6] Han Cai, Chuang Gan, Tianzhe Wang, Zhekai Zhang, and Song Han. Once for all: Train one network and specialize it for efficient deployment. *arXiv preprint arXiv:1908.09791*, 2019.

[7] Rewon Child, Scott Gray, Alec Radford, and Ilya Sutskever. Generating long sequences with sparse transformers. *arXiv preprint arXiv:1904.10509*, 2019.

[8] Krzysztof Choromanski, Valerii Likhosherstov, David Dohan, Xingyou Song, Andreea Gane, Tamas Sarlos, Peter Hawkins, Jared Davis, Afroz Mohiuddin, Lukasz Kaiser, et al. Rethinking attention with performers. *arXiv preprint arXiv:2009.14794*, 2020.

[9] Tri Dao. Flashattention-2: Faster attention with better parallelism and work partitioning. *arXiv preprint arXiv:2307.08691*, 2023.

[10] Tri Dao, Daniel Y Fu, Stefano Ermon, Atri Rudra, and Christopher Ré. Flashattention: Fast and memory-efficient exact attention with io-awareness. *Advances in Neural Information Processing Systems*, 2022.

[11] Epoch AI. Trends in training dataset sizes. *Epoch AI Report*, 2023. Available at: `https://epochai.org/`.

[12] Elias Frantar, Saleh Ashkboos, Torsten Hoefler, and Dan Alistarh. Gptq: Accurate post-training quantization for generative pre-trained transformers. *arXiv preprint arXiv:2210.17323*, 2022.

[13] Song Han, Huizi Mao, and William J Dally. Deep compression: Compressing deep neural networks with pruning, trained quantization and huffman coding. *arXiv preprint arXiv:1510.00149*, 2015.

[14] Jordan Hoffmann, Sebastian Borgeaud, Arthur Mensch, Elena Buchatskaya, Trevor Cai, Eliza Rutherford, Diego de Las Casas, Lisa Anne Hendricks, Johannes Welbl, Aidan Clark, et al. Training compute-optimal large language models. *arXiv preprint arXiv:2203.15556*, 2022.

[15] Jia-Wei Hong and H. T. Kung. I/o complexity: The red-blue pebble game. *Proceedings of the 13th Annual ACM Symposium on Theory of Computing*, pages 326–333, 1981.

[16] Itay Hubara, Matthieu Courbariaux, Daniel Soudry, Ran El-Yaniv, and Yoshua Bengio. Quantized neural networks: Training neural networks with low precision weights and activations. *The Journal of Machine Learning Research*, 18(1):6869–6898, 2017.

[17] Angelos Katharopoulos, Apoorv Vyas, Nikolaos Pappas, and François Fleuret. Transformers are rnns: Fast autoregressive transformers with linear attention. *International Conference on Machine Learning*, pages 5156–5165, 2020.

[18] Younggyo Kim, Seunghyun Woo, Dongjun Shin, and Kimin Kim. Lipschitz continuity in model-based reinforcement learning. *International Conference on Machine Learning*, 2021.

[19] Nikita Kitaev, Łukasz Kaiser, and Anselm Levskaya. Reformer: The efficient transformer. *arXiv preprint arXiv:2001.04451*, 2020.

[20] Andrei N Kolmogorov and Vladimir M Tikhomirov. ε-entropy and ε-capacity of sets in functional spaces. *American Mathematical Society Translations: Series 2*, 17:277–364, 1959.

[21] Rolf Landauer. Irreversibility and heat generation in the computing process. *IBM Journal of Research and Development*, 5(3):183–191, 1961.

[22] Ji Lin, Jiaming Tang, Haotian Tang, Shang Yang, Xingyu Dang, and Song Han. Awq: Activation-aware weight quantization for llm compression and acceleration. *arXiv preprint arXiv:2306.00978*, 2023.

[23] Hao Liu, Matei Zaharia, and Pieter Abbeel. Ring attention with blockwise transformers for near-infinite context. *arXiv preprint arXiv:2310.01889*, 2023.

[24] James Martens. New insights and perspectives on the natural gradient method. *Journal of Machine Learning Research*, 21(1):5776–5851, 2020.

[25] Yurii Nesterov. *Lectures on Convex Optimization.* Springer, 2018.

[26] Noam Shazeer. Fast transformer decoding: One write-head is all you need. *arXiv preprint arXiv:1911.02150*, 2019.

[27] Daniel A Spielman and Nikhil Srivastava. Graph sparsification by effective resistances. *SIAM Journal on Computing*, 40(6):1913–1926, 2011.

[28] Susanne Still, David A Sivak, Anthony J Bell, and Gavin E Crooks. Thermodynamics of prediction. *Physical Review Letters*, 109(12):120604, 2012.

[29] Sinong Wang, Belinda Z Li, Madian Khabsa, Han Fang, and Hao Ma. Linformer: Self-attention with linear complexity. *arXiv preprint arXiv:2006.04768*, 2020.

[30] David H Wolpert. The stochastic thermodynamics of computation. *Journal of Physics A: Mathematical and Theoretical*, 52(19):193001, 2019.

[31] Yunyang Xiong, Zhanpeng Zeng, Rudrasis Chakraborty, Mingxing Tan, Glenn Fung, Yin Li, and Vikas Singh. Nyströmformer: A nyström-based algorithm for approximating self-attention. *AAAI Conference on Artificial Intelligence*, 35(16):14138–14148, 2021.

[32] Manzil Zaheer, Guru Guruganesh, Kumar Avinava Dubey, Joshua Ainslie, Chris Alberti, Santiago Ontanon, Philip Pham, Anirudh Ravula, Qifan Wang, Li Yang, et al. Big bird: Transformers for longer sequences. *Advances in Neural Information Processing Systems*, 33:17283–17297, 2020.